STRAIN ENGINEERING AS A METHOD FOR MANUFACTURING MICRO- & NANO- SCALE RESPONSIVE PARTICLES

A Thesis
Presented to
The Academic Faculty

by

Brian Keith Simpson, Jr.

In Partial Fulfillment
of the Requirements for the Degree
Master of Science in the
School of Mechanical Engineering

Georgia Institute of Technology
August 2010

STRAIN ENGINEERING AS A METHOD FOR MANUFACTURING MICRO- & NANO- SCALE RESPONSIVE PARTICLES

Approved by:

Dr. Kyriaki Kalaitzidou, Advisor
School of Mechanical Engineering
Georgia Institute of Technology

Dr. Karl I. Jacob
School of Polymer, Textile & Fiber Engineering
Georgia Institute of Technology

Dr. Peter J. Hesketh
School of Mechanical Engineering
Georgia Institute of Technology

Date Approved: [Date Approved by Committee]

ACKNOWLEDGEMENTS

This thesis is the compilation of 1 1/2 years of research that began when I accepted a position as a graduate research assistant in Dr. Kyriaki Kalaitzidou's research group at the Georgia Institute of Technology. In this time, I have had the pleasure of advancing my skills as a mechanical engineer and embark upon a path as a researcher where I was able to develop new ideas and contribute to subjects that I truly have a passion for.

I would like to first thank God for bestowing upon me the abilities to achieve the things I have been able to achieve thus far in my life. I would like to also thank my parents Brian & Angela Simpson and grandparents Gloria & Joseph Cormier whose love and guidance have made me the person that I am today. It is through their teachings and support that I have remained humble and respectful to all of the individuals who have walked in and out of my life.

I owe my deepest gratitude to my supervisor, Dr. Kyriaki Kalaitzidou, for taking a chance and believing in my abilities to succeed. It was her encouragement, guidance and support that allowed me to push forward in times of self-doubt and overcome obstacles that seemed insurmountable at times. It was truly an honor for me to work with her on several projects because of the vast amounts of knowledge I was able to gain during her caring and patient approach to developing me into a graduate student. For this, I will forever consider Dr. Kalaitzidou a great friend and advisor.

I am indebted to my many colleagues who have supported me over the years. Dr. Wanda Jones provided me with my first experiences in research as an undergraduate research assistant at Tuskegee University. It was during this time that the idea of

graduate school began to cross my mind. I would like to acknowledge Grady Nunnery, Christopher Tzanavaris, Kathleen Anderson, Handoko Santoso, Andrea Marcon and Xiaohui Lin for their contributions to the research discussed in this thesis. I would also like to acknowledge my research group members Md Atiqur Bhuiyan, Mehdi Karevan and Chun Chu for the cheerful and enlightening times spent in our graduate office. Even during the busy times in the semester, we always found the time to talk, laugh and learn about each other's cultures. I would hope that as the only native of the U.S. in our office that I made their time away from home worthwhile. I would also like to thank Tina Chang for her patience with me as well as continuing to offer her advice and support even during the hectic times. She provided the confidence and motivation that I needed to always work hard and try my best. Finally, I would like to show my appreciation to campus organizations such as the Black Graduate Student Association (BGSA), the National GEM Consortium and Facilitating Academic Careers in Engineering and Science (FACES) for not only what they have done for me, but what they have and continue to do for under-represented individuals across the nation. It is through all of these experiences that I have acquired throughout my life and in the last year and a half that have prepared me in writing this thesis.

TABLE OF CONTENTS

	Page
ACKNOWLEDGEMENTS	iii
LIST OF TABLES	viii
LIST OF FIGURES	ix
SUMMARY	x
CHAPTER 1: INTRODUCTION	1
1.1 Strain Engineering	2
1.2 Rigid Structures Made by Strain Engineering	3
1.3 Responsive Structures Made by Strain Engineering	6
1.4 Mechanics of Bi-Layer Heterostructures	12
1.5 Objectives	16
CHAPTER 2: RESPONSIVE PARTICLES: MATERIALS & FABRICATION	18
2.1 Material Selection	19
2.1.1 Sacrificial Layer	20
2.1.2 Elastomeric Substrate	20
2.1.3 Top Thin Films	21
2.2 Preparation of PDMS Layer	25
2.2.1 Controlling PDMS Thickness	25
2.2.2 Controlling PDMS Modulus	28
2.2.3 Controlling Uniform Mismatch Strain	29
2.3 Deposition of Top Film Layer	30
2.4 Lateral Cutting of the Bi-Layer	33

2.5 Triggering the Response 39

CHAPTER 3: CHARACTERIZATION OF RESPONSIVE PARTICLES 43

3.1 Characterization Tools & Methods 43

3.1.1 Characterization of Modulus 44

3.1.2 Characterization of Thickness 45

3.1.3 Characterization of the Radius of Curvature 46

3.2 Results of Modulus Characterization 46

3.3 Results of Thickness Characterization 48

3.4 Results of the Radius of Curvature Characterization 49

3.5 Au/Ti Film Deposition Rate 51

3.6 Material System Evaluation 53

CHAPTER 4: DEMONSTATION OF THE REVERSIBLE RESPONSIVE PARTICLE BEHAVIOR 57

4.1 Rheological Method 57

4.2 Light Intensity 60

4.3 Capture/Release Ability of Thermo-Responsive Particles 62

CHAPTER 5: LARGE-SCALE MANUFACTURING OF RESPONSIVE PARTICLES 66

5.1 Implementing a Systematic Design Approach 67

5.1.1 Gap Analysis 68

5.1.2 Modification Proposal 70

5.2 PDMS Preparation 75

5.3 Layer Deposition 77

5.4 Curing 79

5.5 Cutting 79

5.6 Removing the Sacrificial Layer 81

CHAPTER 6: RESPONSIVE SURFACES 82

6.1 Strain Sensors 82

6.2 Strain Sensor Fabrication 84

6.3 Strain Sensor Characterization 86

CHAPTER 7: CONCLUSIONS 95

7.1 Findings 95

7.2 Limitations & New Challenges 100

REFERENCES 102

LIST OF TABLES

	Page
Table 2.1: Top thin film materials and stimuli	22
Table 2.2: PDMS Thickness Testing Parameters	26
Table 2.3: PDMS/Hexane ratios	28
Table 2.4: PDMS curing temperature test	29
Table 2.5: Processing Parameters of Top Film Layers	33
Table 3.1: Effect of curing temperature on PDMS modulus	47
Table 3.2: Effect of modulus on particle diameter	48
Table 3.3: PDMS layer profilometer data	49
Table 3.4: Effect of processing parameters on interfacial strain	51
Table 3.5: Property comparison between top film layer materials	56
Table 4.1: Densitometric Mean Values	61
Table 5.1: Gap Analysis - planning & clarification of task	69
Table 5.2: Gap Analysis – developing the concept	70
Table 5.3: Working principle chart	73
Table 5.4: Selection chart	74
Table 6.1: The effect of VGCF concentration on composite modulus	86
Table 6.2: The effect of VGCF concentration on composite electrical resistance	89

LIST OF FIGURES

Page

Figure 1.1: Localized film rupture/de-bonding in metal film/substrate structures under tensile strain 8

Figure 1.2: Effect of a compliant substrate on necking 8

Figure 1.3: Visualization of the influence of thin film stresses on the curvature 11

Figure 1.4: Adaptive polymer particle fabrication process 12

Figure 1.5: Bi-Layer structure schematic 14

Figure 2.1: Manufacturing Process 18

Figure 2.2: Parylene-PDMS bi-layer response 23

Figure 2.3: Film thickness vs. hexane dilution 27

Figure 2.4: Effect of curing on PDMS layer 30

Figure 2.5: Unaxis PECVD System 31

Figure 2.6: (Left) Gold Sputtering Unit (Right) CVC E-Beam Evaporator 32

Figure 2.7: Laser-cut thin polymer SEM image 35

Figure 2.8: Effects of laser cutting 36

Figure 2.9: Micro-machining cutting surface 37

Figure 2.10: Micromachining cutting job with different tool sizes 38

Figure 2.11: Stress within the bi-layer structure 39

Figure 2.12: Effect of applying/removing stimulus 40

Figure 3.1: Particle thickness SEM image 49

Figure 3.2: Effect of curing temperature on PDMS modulus & particle size 50

Figure 3.3: Au/Ti deposition rate vs particle diameter 53

Figure 3.4: Comparing particles for two material systems 55

Figure 4.1: Viscosity of Si oil 59

Figure 4.2: Viscosity of Si oil with particles 59

Figure 4.3: Light Intensity Images 61

Figure 4.4: Partial/Complete PEG-FITC absorption 63

Figure 4.5: Capture/Release ability of responsive particles 64

Figure 5.1: Affinity diagram 71

Figure 5.2: Function Structure Diagram 72

Figure 5.3: Automated PDMS preparation approach 77

Figure 5.4: Large-scale manufacturing conveyor concept 78

Figure 5.5: Automated micro-drilling tool 80

Figure 6.1: PDMS-VGCF strain sensor mechanism 83

Figure 6.2: Manufacturing process for PDMS/VGCF thin films 85

Figure 6.3: Strain sensor holding apparatus 88

Figure 6.4: Effect of VGCF concentration on tensile modulus and resistance of a composite 90

Figure 6.5: Effect of strain on the electrical conductivity of a composite material 91

Figure 6.6: Effect of VGCF concentration and cross-linking agent ratio on tensile modulus 92

Figure 6.7: Effect of cross-linking agent ratio on electrical resistance for 3% VGCF 93

SUMMARY

Strain engineering is used as a means of manufacturing micro- and nano- scale particles with the ability to reversibly alter their geometry from three dimensional tubes to two dimensional flat layers. These particles are formed from a bi-layer of two dissimilar materials, one of which is the elastomeric material polydimethylsiloxane (PDMS), deposited under stress on a sacrificial substrate. Upon the release of the bi-layer structure from the substrate, interfacial residual stress is released resulting in the formation of tubes or coils. These particles possess the ability to dramatically alter their geometry and, consequently, change some properties that are reversible and can be triggered by a stimulus. This work focuses on the material selection and manufacturing of the bi-layer structures used to create the responsive particles and methods for characterizing and controlling the responsive nature of the particles. Furthermore, the potential of using these particles for a capture/release application is explored, and a systematic approach to scale up the manufacturing process for such particles is provided. This includes addressing many of the problems associated with fabricating ultra-thin layers, tuning the size of the particles, understanding how the stress accumulated at the interface of a bi-layer structure can be used as a tool for triggering a response as well as developing methods (i.e. experiments and applications) that allow the demonstration of this response.

CHAPTER 1

INTRODUCTION

The purpose of this study is to examine how strain engineering can be used to manufacture three-dimensional responsive polymer particles on a micro- and nano- scale. This study will focus on the material selection and manufacturing of thin bi-layer structures used to create three-dimensional particles and methods for their characterization. This study will also focus on demonstrating/controlling the responsive nature of the particles through experimentation and novel applications as well as discussing approaches to scaling up the manufacturing process of these objects. This includes addressing many of the problems associated with manufacturing ultra-thin layers and understanding how the stress accumulated at the interface of a bi-layer structure can be used as a tool for triggering a response. There are many issues surrounding the manufacturing of the thin bi-layer structure such as choosing which materials will compose the bi-layer structure, determining the appropriate thickness of each layer, depositing the layers, curing and cutting the materials involved as well as triggering the response. Each of these issues will be discussed in detail. Additionally, the various mechanical properties of the materials and well-known techniques for measuring the modulus, stress, strain and viscosity will be addressed.

In order to create responsive particles, it is necessary that one or both of the layers in the bi-layer structure possess material properties that allow the material to reversibly alter its geometry and thus its properties in a controllable fashion. It is for this reason that one layer in the bi-layer structure is made of an elastomeric material, polydimethylsiloxane (PDMS), which is conducive to forming structures that are

responsive and will not fail over several repeated cycles. The idea of using an elastomeric material in this study makes this work unique from typical layered structures made of rigid materials because the rigid bodies do not have the ability to change and return back to their previous state. This prevents these materials from being viable controlled-response candidates. The second material of the bi-layer, referred from this point on as the film layer, does not necessarily have to be an elastomeric material, but usually consists of a material with at least one property that differs vastly from PDMS. It is this difference in the property of the two materials that can be exploited by applying the proper stimulus. If the change that is occurring in each material is large enough, a case of misfit strain can transpire leading to the development of interfacial residual stress. It is this residual stress that initiates the response of the bi-layer structure and will serve as the underlying principle in how this process works.

1.1 Strain Engineering

Strain engineering is a strategic process that involves using mechanical strain as a manufacturing tool that can be used in an effort to control material performance by changing certain properties within the material. Strain engineering which is most commonly used as a method to increase the carrier mobility in the active regions of advanced transistor devices and the manufacturing of semiconductors [1-3] has been adopted in this research due to the fact that many of the behavioral characteristics that embodies this work are similar to those used in semiconductor manufacturing and many of the discoveries made by many of these research groups who have performed such analysis have laid the groundwork for the research that will be discussed. In this case, strain engineering is the strategy employed to utilize the residual stress developed at the

interface of bi-layer heterogeneous structures bonded to a glass substrate by a sacrificial layer. The residual stress that develops at the interface is due to lattice-misfit strain between layers that is caused by variations in thermal expansion rates or other factors such as exposure to solvents, electrical current and UV radiation that could affect one layer in the bi-layer differently from the other. When this interfacial stress is released upon de-bonding of the structure from the substrate, the formation of three-dimensional micro- and nano-objects occurs [4-6].

The next sections will examine how strain engineering plays an important role in altering the physical properties of structures made from both rigid and compliant materials as well as how strain engineering can be used as a tool to control residual stress in layered heterostructures. In both cases, detailed experimental techniques discuss uses for strain engineering in manufacturing which provide the foundation that the current study is intended to build upon.

1.2 Rigid Structures Made by Strain Engineering

Depositing thin, rigid materials under compression or tension in order to make multi-layered heterostructures provides some examples of strain engineering. Strain engineering has found a niche as an approach in improving the performance of rigid semiconducting devices (i.e. transistors). For many cases, techniques used to introduce strain during the fabrication of the rigid structure are used to create new structures that exhibit enhanced properties compared to that of those produced without strain [1-3].

A number of studies were performed using strain engineering to improve carrier mobility in the active regions of advanced transistor devices. In one example, applying strain to Si-based heterostructures was cited as a possible way of enhancing device

performance through changes in the material properties rather than typical methods for enhancement which would involve changing the device geometry or doping [2]. For one study, metal–oxide–semiconductor field-effect transistors (MOSFETs) were fabricated on strained and relaxed $Si_{0,8}Ge_{0,\ 2}$ heterostructures. The devices fabricated by both the strained and unstrained methods were compared, and it was found that MOSFET mobility of the strained-Si device was enhanced by 75% compared to that of the unstrained-Si device [2].

This same idea is presented in the fabrication of high performance and low power integrated circuits (ICs). Here, two strain engineering techniques using silicon-on-insulator (SOI) substrates to further enhance integrated circuit performance are explored. The first procedure tested was the 'local strain' or 'process-induced strain' approach. This procedure is based upon uniaxial strain that is induced during the manufacturing of the semiconductor. The strain is applied through the deposition of nitride spacers or epitaxial SiGe source/drain pockets. The second approach serves as an alternative to the 'local strain' approach known as the 'global strain' approach. This approach involves growing a strained Si layer by hetero-epitaxy on a relaxed $Si_{1-x}Ge_x$ layer to modulate channel strain. The purpose of the relaxed SiGe layer is to enable formation and maintain the strain in the Si layer. Tensile strain is induced in the silicon as the lattice of the silicon layer is stretched to mimic the larger lattice constant of the underlying SiGe. Also, if compressive strain was desired, this could be induced by using a solid solution with a smaller lattice constant, such as silicon-carbon. This strain determines how much the transistor's performance will be enhanced [3]. Despite these breakthroughs, both

approaches pose technical challenges that limit their application in semiconductor manufacturing.

Strain engineering has also been employed in micro-electro-mechanical systems (MEMS) in order to examine internal stresses that develop in thin films. Researchers that study MEMS understand how developing the ability to control stress in thin films is critical in managing the performance, reliability and long-term stability of most micromechanical, electronic, magnetic or optical devices where thin films are used. For example, two experimental techniques were performed to analyze the residual stress in low-temperature plasma enhanced chemical vapour deposited (PECVD) SiNx thin films [1]. The first measured the stress-induced substrate curvature, while the other took advantage of stress-induced deformation of freestanding microstructures. This study focused on major influences of stress in thin films during deposition. The study discussed how thin film materials deposited under stress want to return back to equilibrium by relieving stress. In order for a film deposited in under compression to reach equilibrium, the molecules that make up the material must spread apart in order to return to equilibrium. Consequently, if the film is attached to a substrate, this stress relaxation will result in the bending of the substrate concave down. Alternatively, if the deposition of the thin film results in tension, the opposite is true meaning the molecular particles in the material are spread further apart. In this case, the movement of the particles to their equilibrium position results in the relaxation of this stressed state causing bending of the substrate concave up.

Theoretically, the more stress that the film is under when deposited, the more it would want to bend. Using this idea, studies that were performed on thin films

determined that by measuring the substrate's radius of curvature, the presence and magnitude of the stress in the deposited thin film could be measured. The thin film stress was later quantified using an equation derived from Stoney's formula [7],

$$\sigma_f = E_s/(6R\,(1-\nu_s)) * d_s^2/d_f \quad (1)$$

where E_s, ν_s, and d_s are Young's modulus, Poisson ratio, and thickness of the substrate, respectively, R is the experimentally obtained substrate's radius of curvature, and d_f is the thickness of the thin film [1]. The equation developed above assumes the following are true:

1. Only stress values averaged over a large surface area of several square centimeters can be determined
2. Stress values are dependent on the uniformity of the film layer on the substrate
3. The substrate is thicker than the film layer

The same study also discussed introducing a sacrificial layer in between the substrate and film layer as a method of measuring stress in suspended thin films that deform without introducing any substrate bending [1]. Of the many benefits that came out of this analysis, one of the major conclusions was that the temperature during deposition is a major factor in determining the amount of residual stress in a thin film.

1.3 Responsive Structures Made by Strain Engineering

For over a decade, several research groups have pioneered the idea of using compliant substrates as a means of producing electrical circuits that are flexible, stretchable and compressible. These compliant electrical surfaces have been designed for

applications ranging from medical health monitors to flexible circuit boards. In each of these applications, principles of strain engineering were devised.

Significant strides in the development of flexible circuits that work in both a stretched and compressed state were achieved in recent studies. It is already well understood that sub-circuits can be electrically connected with stretchable metal conductors. One group outlined three options for making deformable interconnects: making thin metal films that can withstand large plastic deformation, deforming a sacrificial mask that then serves in liftoff metallization, and making stretchable metallization. In analyzing the three options, information on thin film deposition, electrical/mechanical properties of thin films, and manufacturing techniques were gathered [8-10]. For example, free standing metal films can only stretch by 1%-2% before they rupture. This is the result of necking at its weakest cross-section. Once the necking begins, the strain in the metal film localizes at the neck while the rest of the metal stretches relatively little. As a result, the rupture strain is quite small. To prevent this, it is essential that the metal film is bonded well to a compliant substrate (i.e. rubber/PDMS) as shown in Figures 1.1 and 1.2 below [10-12]. Meanwhile, metal films bonded to an elastomeric substrate can remain electrically conducting even under large and repeated stretching and relaxation.

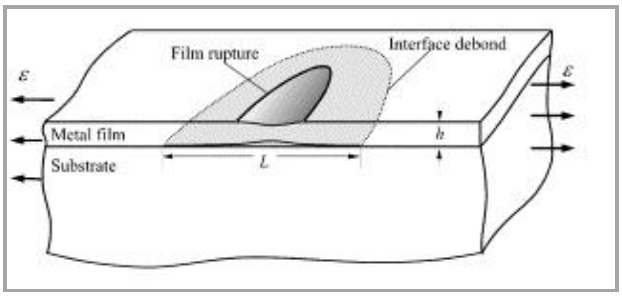

Figure 1.1: Localized film rupture/de-bonding in metal film/substrate structures under tensile strain [11]

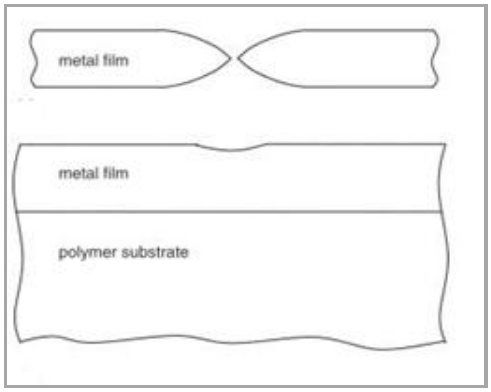

Figure 1.2: Effect of a compliant substrate on necking [11]

It was found that many metal films fatigue quickly if subjected to cyclic loading. However, a metal film on an elastomeric substrate can be stretched repeatedly by tens of percent over hundreds of cycles without fatigue and remain electrically conducting [13]. The same holds true in bi-layer structures if the film and substrate de-bond over a length much larger than the film thickness. The film becomes free-standing and will rupture by localized deformation under small strains. This explains why in many cases surface cracks and deformities can be found in bi-layer structures [8]. It was later discovered that the delamination of the thin film was caused by the out-of-plane deflection of the film. In addition to this, the distributed micro-cracks caused by this delamination did not disrupt the thin film's ability to avoid fatigue and sustain cyclic stretching [8]. Two factors: the micro-scale structure of the film and the compliance of the substrate are used to explain

why this phenomenon occurs. One study verified that a stiff material film can be made elastically stretchable if the film is suitably patterned. This is justified by cutting patterns in a large piece of aluminum foil and analyzing how the foil behaves when strained. In associating the foil experiment with the compliance of the substrate, it was shown that if the substrate were stiff, it would confine the deformation of the film in its plane. In contrast, a sufficiently compliant substrate (e.g. PDMS) allows the microscopically patterned film to deform almost like the freestanding transparency foil: by deflecting and twisting out of the plane [13]. The same group demonstrated that Au film deposited onto an elastomeric substrate with built-in compressive stress can maintain electrical conductivity up to 22% tensile strain [9]. Using metal films in the bi-layer structure opens the door for possible electronic applications by utilizing the electrical conductive properties of the film layer. In combination with the elastomeric layer, these conductive films can now withstand high strain and will not fatigue, leading the way for stretchable electronics.

An approach used to design these elastic circuits was achieved by distributing rigid sub-circuit islands over a polymer surface and, then, fabricating active devices on the islands. The islands need to be interconnected with stretchable metallization. The first elastic circuit developed by this method was an inverter of thin film transistors. The circuit remained functional when stretched and relaxed by 12% strain [10]. The significance of these findings have opened the door to enabling electro-active surfaces of arbitrary shape wrapped over airplane wings, buildings, robots, three-dimensional (3-D) displays, and human medical prostheses. These large surfaces will sense physical

parameters such as temperature, pressure, or flow, will be electrically powered and controlled, and will assess their condition and environment, and respond to it [10].

The idea of stretchable electronics was taken in different directions in various studies. One study found that analytical and finite element method (FEM) simulation of the mechanics together with circuit simulations reveal the key physics of film and substrate behavior [12]. In addition to the technology used above, elementary bending mechanics was utilized to understand how these material structures can offer end-to-end stretchability and compressibility in brittle materials. Researchers noticed that since the elastic modulus of the PDMS substrate is several orders of magnitude smaller than that of Au film, the effect of interface shear is negligible in his mechanical analysis. This conclusion was verified in a study using finite element analysis [14]. It is noted that one disadvantage of thin/stiff films on complaint wavy substrates is that compressive strains in the buckled films, established in the manufacturing procedures, yield stretchability at the expense of reduced compressibility [14]. An approach would later be developed that patterned silver electrodes by omnidirectional printing of concentrated nanoparticle inks that can withstand repeated bending and stretching to large levels of strain with minimal degradation of their electrical properties [15].

Perhaps the most intriguing use of strain engineering with responsive materials is the creation of free-standing particles. This ideology was put into practice for the creation of free-standing ‘nanopipelines’ that were fabricated using SiGe-based epitaxial layers grown on a Ge sacrificial layer bonded to a Si substrate [16]. Selective etching of the sacrificial layer results in the bending of the bi-layer structure and the formation of nanopipelines. This example was visualized in the Figure 1.3 below.

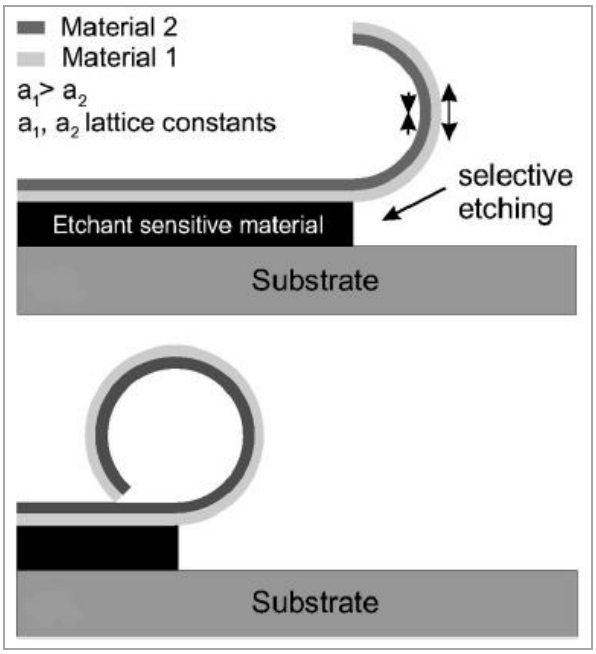

Figure 1.3: Visualization of the influence of thin film stresses on the curvature [16]

A similar process for manufacturing responsive polymer-based particles was created from bi-layer structures composed of PDMS and a Au/Ti film layer. This bi-layer structure was built upon a sacrificial layer that bonded the bi-layer structure to a substrate. As seen in Figure 1.4 below, this process eventually produced micro-sized tubes and coils that are formed as a result of the relaxation of the residual thermal stress that develops at the interface of the bi-layer [17].

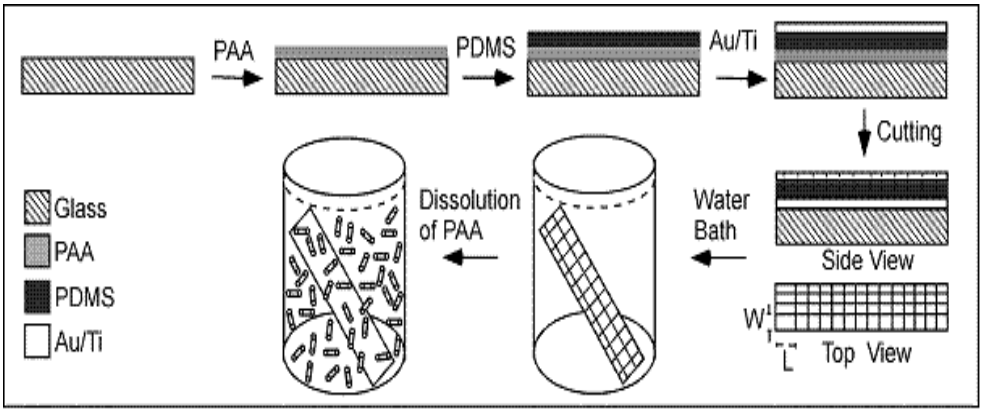

Figure 1.4: Adaptive polymer particle fabrication process [17]

For the manufacturing process covered in this thesis, the basic principles of this method will remain the same, but in an effort to expand the knowledge gained on how each component of the manufacturing process affects the final product, experimental set-ups to test the bounds of the process have been established. Processing parameters such as curing temperature, layer thickness and cutting strategies will be explored in order to discover key variables that contribute to the size and mechanical behavior of the particles. Before beginning the manufacturing process for the bi-layer heterostructures in this study, there is a need to understand the mechanics of the bi-layer.

1.4 Mechanics of Bi-Layer Heterostructures

In dealing with structures that are bending and curving under stress, it can be assumed that the thin-layered responsive material follows the same basic mechanical principles as that of the single or multi-layered cantilever beam. In reality, this is not the case. Due to the thicknesses of thin films, generally being in the micro- and nanometer range, their thermomechanical properties might differ from those of bulk materials [18].

In an effort to solve this problem, one researcher developed a formula that would serve as the basis for experimental work on stress measurement in thin films bonded to substrates [7]. In its most basic form, the formula provides an expression for the curvature (κ) of the substrate in terms of the residual force (f) in the film (interpreted as a force per unit distance along the interface) due to misfit and/or other residual elastic strain. This expression is written as:

$$\kappa_{St} = 6f/h_s^2 M_s \qquad (2)$$

where h_s and M_s are the thickness and the biaxial elastic modulus of the substrate, respectively. The formula above is based on several assumptions that include [19]:

1. The thickness of both the film and substrate are small compared to the lateral dimensions
2. The film thickness is much less than the substrate thickness
3. The substrate material is homogeneous, isotropic, and linearly elastic
4. The film material is isotropic
5. Edge effects near the periphery of the substrate are inconsequential and all physical quantities are invariant under change in position parallel to the interface
6. All stress components in the thickness direction vanish throughout the material
7. The strains and rotations are infinitesimally small

Though many of these assumptions make sense in the typical experimental set-up, this formula's validity has been tested at various extremes to verify its effectiveness in a variety of situations. Research on the mechanics of bi-layer structures has led to many augmentations and expansions to the formula as well as the amendment of some assumptions. In one study, an analysis of the film/substrate bi-layer and multilayer deflection due to lattice mismatch was presented. Though this work, it was concluded that the assumption of a uniform curvature is not valid for large nonlinear deformations [19]. Additionally, another group was able to examine two different models of the film/substrate system which prove that the assumption of a uniform curvature is not valid even in the case of small linear deflections if there are in-plane forces. Physically, thermal and intrinsic stresses due to film growth are the two major sources of in-plane

stresses and forces. This led to the conclusion that in the absence of in-plane force, uniform curvature is always valid for small deflections [20].

In many of these studies, basic derivations are provided relating classic mechanics and strength of materials to the principles embedded in the Stoney formula. For instance, one group performed basic analysis of a classic film-substrate bi-layer system. The film-substrate bi-layer structure was formed by depositing a thin film of thickness t_f onto a substrate of thickness t_s as shown in Figure 1.5:

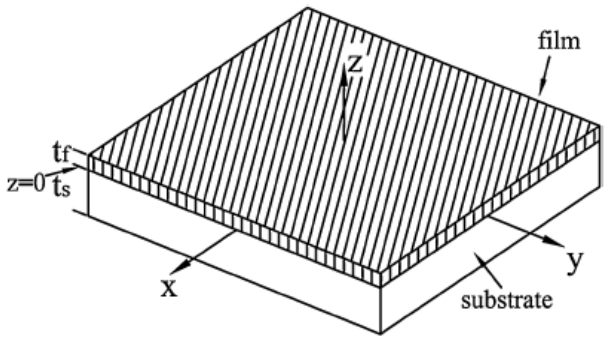

Figure 1.5: Bi-Layer structure schematic [18]

As the deposition temperature is higher than the room temperature by ΔT, the mismatch in coefficients of thermal expansion between the film and substrate causes the bi-layer structure to bend [18]. Other groups focused on deriving variables that contributed to the behavior of the bending surface which included equations for defining the lattice mismatch strain acting on the film and substrate layers. Based on Newton's third law, these equations indicate that if the strain in one layer is negative, the other has to be positive. This implies that there is a bending moment due to mismatch strain and film/substrate system is subject to bending deformation [20]. In addition to the bi-layer strain analysis, equations were developed that opened the door to the understanding of

how interfacial stress, modulus, and thickness fits into this analysis. These equations are key in developing test set-ups that will allow the exploration of each variable's effect on the radius of curvature [21].

Combining all of the concepts discussed prior, along with various experiments to validate these assumptions and equations, an expanded form of the Stoney formula was created:

$$\kappa = (6\varepsilon_m/h_s)(hm)[(1 + h)/(1 + hm(4 + 6h + 4h^2) + h^4m^2] \quad (3)$$

where $h = h_f/h_s$ is the film/substrate thickness ratio and $m = M_f/M_s$ is the film/substrate modulus ratio. This is the generalization of the Stoney formula for uniform mismatch strain in a film of arbitrary thickness ratio and arbitrary modulus ratio. The factor outside the square brackets in the equation above is κ_{St} and $\kappa \Rightarrow \kappa_{St}$ as $h \Rightarrow 0$ [19].

From the years of work to amend the original Stoney formula, researchers were able to use the equation for the radius of curvature for bi-layer structures based on an augmented equation which defined the curvature. Since the radius of curvature is the inverse of the curvature, the equation for the radius of curvature was written as [22]:

$$\rho = (h_s/6\varepsilon)[1 + hm(4 + 6h + 4h^2) + h^4m^2]/(hm + h^2m) \quad (4)$$

where $m = (E_f/E_s)[(1 - \nu_s)/(1 - \nu_f)]$. The quantities h_i, E_i, and ν_i are thickness, elastic modulus, and Poisson's ratio, respectively, of the i layer. The strain, ε, is the uniform mismatch strain in the film, defined by the differences in coefficients of thermal

expansion in the materials. It is beneficial that many of the variables in the equation are pre-known or can be easily determined through the use of experimental tools. In the case of determining the strain through the thermal expansion mismatch, the accepted values for the coefficient of thermal expansion for bi-layer materials can be used. The Young's modulus of each layer can be determined through tensile testing and the thickness of each layer can be measured using a profilometer. It is this equation that serves as the cornerstone to research in characterizing thin-layered responsive surfaces and particles. It allows the residual stress to be calculated based on data obtained from empirical analysis used to determine the other variables in the equation such as the modulus, thickness, and the radius of curvature. Through this work, the accuracy of this equation should be verified and provide sound data that will help advance bi-layer behavior characterization and design.

1.5 Objectives

In covering the literature in this study, ideas from the leading research teams in the fields of material science, biomedicine, mechanics, and mathematics were highlighted. Each of these findings served as key components in understanding what makes these particles responsive and what measures need to be taken in order to improve performance. Each provided the basis for understanding the mechanics of thin films and how to incorporate strain engineering in manufacturing techniques for building bi-layer structures. The valuable insight provided will allow for the customization of polymer-based particles based on detailed characterization methods. In order to customize these structures, this work will attempt to characterize most, if not all, of the factors involved in

predicting the size, shape, and response of the materials that compose the bi-layer. This will be done by completing the following objectives:

- Develop a method for manufacturing bi-layer heterostructures that can be used to create responsive particles that is simple, repeatable and cost effective (Chapter 2)
- Investigate the processing-property relationship in responsive polymer particles made using strain engineering (Chapter 3)
- Demonstrate the particles ability to reversibly alter their geometry and properties in response to a stimulus by means of response experiments and by applying them to novel applications (Chapter 4)
- Propose an approach for the mass production of responsive particles by scaling up the manufacturing process (Chapter 5)

In addition, the concept of strain recovery of an elastomeric material was utilized to design, manufacture and characterize responsive surfaces such as strain sensors (Chapter 6).

CHAPTER 2

RESPONSIVE PARTICLES: MATERIALS & FABRICATION

Stimuli-responsive materials have attracted a lot of attention because of their many potential applications [23-30]. Though significant progress has been made in the design and synthesis of such stimuli-responsive materials, there are still significant challenges that need to be overcome before these structures can reach their true potential and find suitable applications. Many of these challenges are related to understanding which factors contribute to the responsive ability of the materials and how they can be manufactured in a simple and cost effective manner without compromising quality. The manufacturing process employed in this study utilizes the residual stress developed at the interface of planar heterostructures deposited on a sacrificial substrate. The unique feature in this approach is that an elastomeric material is used as one of the layers. The elastomer, PDMS, provides the responsive ability to the resulting particles. Figure 2.1 below displays how this manufacturing process works.

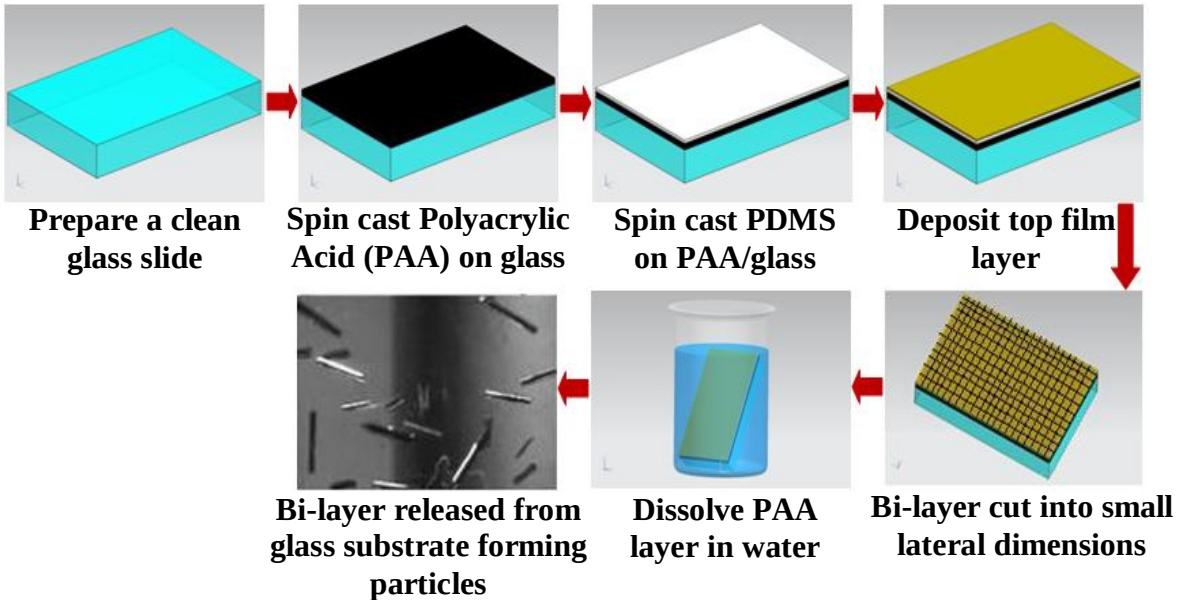

Figure 2.1: Manufacturing Process

This chapter will discuss the materials involved in building the bi-layer structure, techniques for the spin casting and curing PDMS and the deposition of the top film layer. The manufacturing process displayed in Figure 2.1 will address methods for cutting the bi-layer structure in order to create responsive particles. Once the bi-layer structures are built, it will be examined how a stimulus can be used to trigger a response such as a change in geometry or physical properties upon demand.

2.1 Material Selection

The materials used for the fabrication of the responsive particles are polyacrylic acid, PDMS and various top film layer materials. A clean glass surface serves as the substrate for which the materials of the bi-layer structure can be built upon. Next, a thin sacrificial layer made from poly-acrylic acid is deposited. This layer is followed by an elastomeric material, PDMS. It is this layer that gives the bi-layer structure the ability to reversibly alter its shape and physical properties upon demand. The final layer deposited is the top thin film layer. This film layer may consist of an organic or metallic layer given the appropriate qualities.

A good candidate for a film layer needs to possess one or more physical properties that differ vastly from PDMS. For example, to create a responsive structure, the bi-layer can consist a hydrophobic material bonded to a hydrophilic material, a material that responds in a basic solution along with a material that responds in an acidic one, or two materials with vastly different coefficients of thermal expansion. It is easy to see that this property difference plays a large role in what the stimulus for the responsive structure will be. Another stipulation to consider in choosing the film layer is the material's ability to bond closely to the elastomeric layer. Since the structures being

developed are intended to be reversibly responsive, it is important that the film layer is not brittle or prone to delamination from the elastomeric material.

2.1.1 Sacrificial Layer

The purpose of the sacrificial layer is to allow for the release of the bi-layer structure once it is built. Upon removal of the sacrificial the bi-layer structure deforms freely in order to release the residual stress developed at the interface. The material chosen as the sacrificial layer in this process is poly-acrylic acid (PAA 20% wt aqueous solution, Sigma-Aldrich). The reason this material was chosen as the sacrificial layer was due to its solubility in water which provides for a fast, simple and cost-effective way of removing this layer during the manufacturing process. This layer was deposited by means of spin casting. For experimental purposes, the thickness of the PAA layer is irrelevant in that it only determines how long the dissolution of the layer will take, if this process were to be scaled up, the user would want this layer to be as thin as possible in order to reduce the time it would take to release the bi-layer. One important aspect of the deposition process is the uniformity of the PAA layer across the deposition surface. This is important because it ensures that the uniformity of the stress over the deposition area is not compromised.

2.1.2 Elastomeric Substrate

The material that was chosen as the base polymer for the manufacturing of the adaptive polymer particles is PDMS (Sylgard 184^{TM}, Dow Corning Corp.). PDMS is a silicon-based organic polymer. It is very similar to silicon in nature. PDMS is optically clear, non-fluorescent, biocompatible, chemically inert, non-toxic, permeable to gases, non-flammable, and simple to handle and manipulate. In addition to that, it exhibits

isotropic and homogeneous properties, and it is cheaper than silicon [31]. It is easy to handle and polymerize and readily replicates features in a predefined master. Most organic solvents will diffuse into PDMS causing it to swell, but the material is considered to be insoluble in most solvents. Despite this common assumption, recent studies have come about that suggests solvents such as Hexane and Decane can be used to break down PDMS [32].

The polymer is prepared using a pre-packaged elastomer kit provided by the manufacturer that contains a pre-polymer elastomeric base and a cross-linking agent. When combined, these materials form bonds creating a clear, rubbery material. It is recommended by the manufacturer that the elastomeric base and cross-linking agent is mixed at a 10:1 ratio, respectively; in order create a material with the appropriate physical and mechanical properties that the manufacturer intended the material to possess. In the baseline approach for manufacturing these bi-layers, the manufacturer's recommended ratio is followed, but changing this ratio will be considered in order to verify earlier studies and understand how this ratio affects the elastomeric material's modulus and thickness. In addition to adjusting the base-to-cross-linker ratio, it is known that temperature also has an effect on modulus. Since the modulus and thermal expansion of the elastomeric material are critical variables in determining the amount of residual stress in the bi-layer, curing PDMS layers at various curing temperatures was used to examine its effect on the responsive particles that are the result of this process.

2.1.3 Top Thin Films

Four top thin film materials were considered in this study. Each material tested was chosen because they enable the creation of bi-layer structures that vary in the type of

stimulus they respond to. Three of the films examined were organic materials while the fourth material was metallic. The materials used for this study are listed below:

- Parylene C
- Silicon Carbide (SiC)
- Oxidized PDMS
- Gold/Titanium (Au/Ti)

Organic materials are considered appropriate candidates for the film layer due to the wide range of applications these materials can be tuned to perform. Organic materials have been used in past studies in the manufacturing and enhancement of circuits and sensors, biomedicine applications and protective coatings [3, 14, 22, 33]. In addition, organic materials are synthetic and can be synthesized to display properties that are tailored to a specific application. Research involving thin metal films deposited on compliant substrates inspired the idea of using a thin metal film for this step in the process. It was shown that metal films could withstand large deformations when bonded to a flexible material such as the elastomeric layer used in the bi-layer structure [8-10, 12, 13]. In addition, the electrical properties of these metallic layers provide a means of exploring other types of stimuli and applications for the bi-layer structures. Table 2.1 [34] lists the four materials examined in this study along with their respective stimulus.

Table 2.1: Top thin film materials and stimuli

Material	**Coefficient of Thermal Expansion (α) [K^{-1}]**	**Solubility (δ) [$MPa^{1/2}$]**	**Stimulus**
Parylene - C	10.5×10^{-5}	18.0	Solvent
SiC	4×10^{-6}	Highly insoluble	Temperature
Oxidized PDMS	960×10^{-6}	10 – 12.1	Temperature
Au/Ti	14×10^{-6}	Highly insoluble	Temperature

The first material, parylene, is a name given to a family of poly (p-xylylene) polymers produced by a process known as vapor deposition polymerization. Similar to PDMS, Parylene is hydrophobic and biocompatible. Parylene-C, in particular, has been used as a moisture, chemical and dielectric barrier as well as a coating for medical devices, electronics, automotive, military and aerospace applications. In addition, parylene-C offers a material that exhibits both thermal and UV stability [35]. Ultimately, parylene-C was chosen because of its ease of fabrication, chemical stability and its ability to avoid swelling in the presence of solvents. The same cannot be said for PDMS, whose volume can expand to a large extent when placed in such solutions. Figure 2.2 below shows how the parylene-PDMS bi-layer structures alter its shape when placed in a Hexane solution. The difference in swelling between the two materials is the trigger that induces lattice mismatch, thus, causing a strain-induced response to occur in the bi-layer.

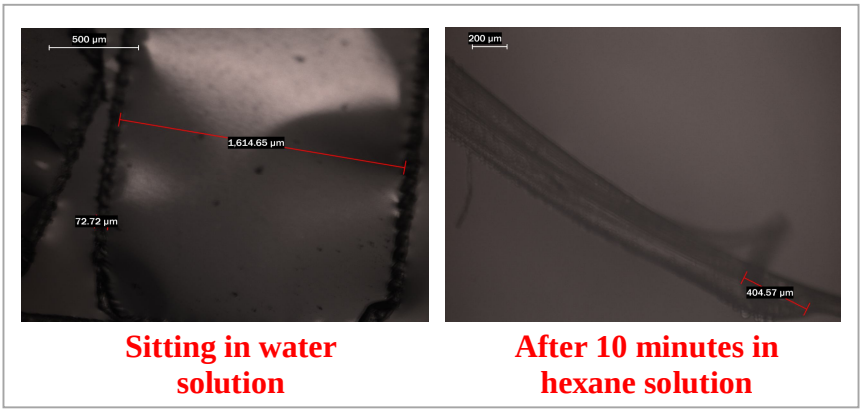

Figure 2.2: Parylene-PDMS bi-layer response

SiC is a chemical compound composed of silicon and carbon. This low-density organic material's hardness and durability have lent it to be used as an abrasive and machining tool since its discovery [36]. Pure SiC is colorless, but it is commonly found in a yellowish-brown color due to impurities. SiC does not melt and experiences sublimation somewhere near 2700 °C [36]. In recent years, SiC has been used as

a semiconducting material in electronics, where its high thermal conductivity, high electric field breakdown strength and high maximum current density make it more promising than silicon for high-powered devices [37]. SiC has a low coefficient of thermal expansion (4.0×10^{-6} K^{-1}) compared to PDMS ($\sim 960 \times 10^{-6}$ K^{-1}) and experiences no phase transitions that would cause discontinuities in thermal expansion [38]. These properties are the primary reasons SiC was chosen as a potential film layer in the bi-layer structure.

The third material tested as a potential top film layer in the bi-layer structure was PDMS itself. This idea is especially favorable since it would not require the actual deposition of another material. Instead, the surface chemistry can be altered by adding silanol (SiOH) groups into to the molecular structure of PDMS through UV or plasma oxidation [1]. When PDMS is oxidized the surface properties change from a hydrophobic material to that of a hydrophilic material essentially forming a new layer that is a few nanometers thick. This ability to change the surface properties of the PDMS bi-layer on command is an important quality for the creation of smart films or surfaces.

Au was the only metal considered for the top film layer because of its malleability, ductility and high electrical conductivity which could lead to many novel applications [8]. The original process for creating responsive polymer particles, in which this manufacturing process is based upon, used a thin layer of Au along with a Ti adhesion layer as the film layer [17]. Like SiC, Au has a low coefficient of thermal expansion (14.0×10^{-6} K^{-1}) compared to PDMS ($\sim 960 \times 10^{-6}$ K^{-1}), but does not form a close bond to PDMS, therefore, metals such as chromium (Cr) or titanium (Ti) are used as adhesive layers between the Au and PDMS to avoid delamination [39].

2.2 Preparation of PDMS Layer

For the deposition of PDMS, steps are needed to prepare the elastomeric material for spin casting. These steps in the manufacturing process are particularly significant because of the important role that the elastomeric layer plays in the responsiveness of the bi-layer structure. The primary goal of these steps is to provide a way to tailor the response and the size of the resulting particles to the application being considered by altering the physical and mechanical properties of the elastomer. In referring back to Eq. 4, it is seen how certain factors control the radius of curvature of the particles that are created from this process. Of the factors outlined in Eq. 4, these steps will be tailored to control:

- Thickness of the PDMS layer
- Modulus of the PDMS layer
- Uniformity and extent of mismatch strain within the bi-layer

To validate the accuracy of Eq. 4, tests that varied these parameters were performed to examine the effect on the radius of curvature. To test these boundaries, various preparation techniques were performed. Processes that involved diluting the PDMS solution as well as increasing spin casting speeds were used to create thinner layers. Also, it was found that curing temperature could be used as a tool to change the modulus and mismatch strain of the elastomeric layer.

2.2.1 Controlling PDMS Thickness

Spin casting is a common micro-manufacturing method for producing polymer films of controlled and uniform thickness [40]. Due to its proven reliability, the 400 Lite Spinner (Laurell Technologies) was used in this manufacturing process [22]. In this step,

degassed PDMS solution (elastomeric base to cross-linking agent ratio 10:1) is poured onto the PAA-coated glass substrate and placed into the spin casting chamber. To analyze the effect of spin rate on the thickness of the deposited layer, the spin casting time is kept constant at 3 minutes while the spin rate is varied from 3000 – 5000 rpm. The resulting thicknesses of these spin rates were measured by profilometer. As expected, the results presented in detail in chapter 3 confirm the decrease in the layer thicknesses as the spin rate is increased.

Table 2.2: PDMS Thickness Testing Parameters

Factors	**Range**
Spin Rate (RPM)	3000, 4000, 5000
PDMS Concentration	100% , 50%

Techniques for fabricating ultra-thin layers using PDMS were examined in this study. This has proven to be a very difficult task because spin casting is limited by the maximum spin rate of the apparatus and PDMS is not soluble in most solvents. In previous attempts, PDMS layer deposition was limited to a minimum layer thickness of ~10 microns [17]. Recent studies suggest that solvents such as Hexane and Decane can be used to break down PDMS [41]. A method was developed for making ultra-thin PDMS membrane devices. By diluting the PDMS (elastomeric base to cross-linking agent ratio 10:1) in hexane (ACS grade, Fisher Scientifics), membranes as thin as ~70 nm were fabricated as shown in Figure 2.3 below.

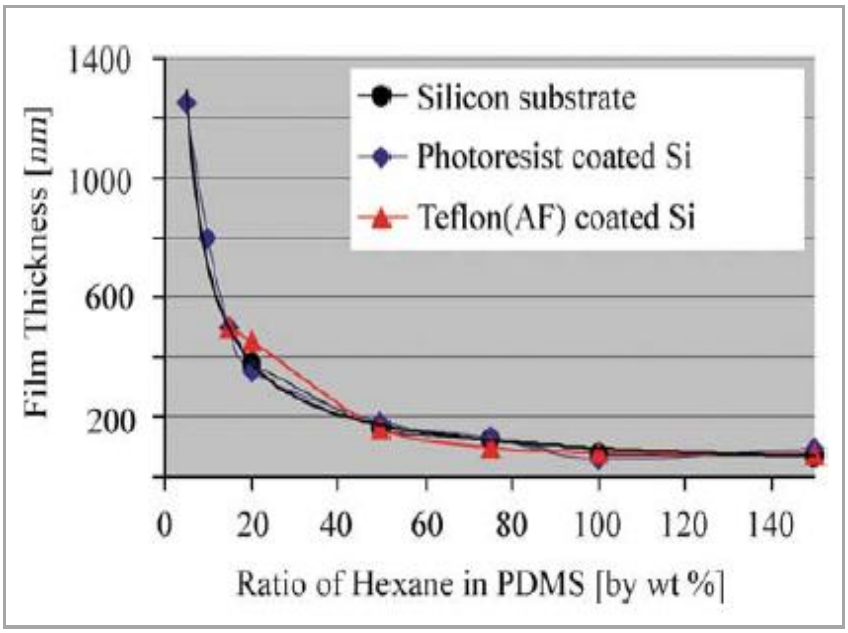

Figure 2.3: Film thickness vs. hexane dilution [41]

In this process the spin rate and duration was kept constant at 6000 rpm and 150 s, respectively [41]. This approach was adopted for the manufacturing of the bi-layer in this study in order to create much thinner elastomeric layers. This would not only improve the flexibility and compressibility of the responsive structures but also allow the structures to produce much smaller particles upon bending that can be utilized in more specialized applications.

To test this technique, batches of PDMS solution were mixed with increasing amounts of Hexane as shown in Table 2.3 below. For this process, the spin rate and duration was kept constant at 4000 rpm and 150s, respectively. Five samples were prepared for each solution and the thickness of each was determined using a profilometer. The results the results presented in detail in chapter 3 confirm the decrease in the layer thicknesses as the spin rate is increased. These results verified that increasing the spin rate along with diluting the solution are viable approaches to creating controlled and uniform thin layers using PDMS.

Table 2.3: PDMS/Hexane ratios

PDMS Weight Pct.	Hexane Weight Pct.
100	0
70	30
50	50

2.2.2 Controlling PDMS Modulus

In studying the mechanical properties of the elastomeric layer, it was found that two factors can be used to control the modulus of PDMS:

- Dilution
- Curing temperature

Diluting the PDMS solution can be used to reduce the density of cross-links and thus, the modulus in addition to decreasing the thickness of the deposited film. In order to examine the effect of dilution on the material modulus, tensile test specimens were prepared using the 100% PDMS and 50% PDMS solution bases shown in Table 2.4. As expected, the PDMS films made by the diluted PDMS have a lower modulus than undiluted PDMS.

In addition, the modulus of PDMS can be increased or decreased by simply changing the temperature at which the material is cured. It is for this reason that curing is a crucial step in the manufacturing process. Typical PDMS curing set-ups are similar in nature unless trying to test the extremes such as high temperature or extended curing times [31]. In this process, a Labline vacuum oven (Thermo Scientific^{TM}) was used to cure the PAA and PDMS layers. In order to test the effect of dilution and curing temperature on the modulus and radius of curvature of the responsive particles, the preparation of PDMS varied according to Table 2.4. The results were able to confirm

that increasing curing temperature increased the modulus of the PDMS which plays a critical role in the size of the particles.

Table 2.4: PDMS curing temperature test

PDMS Weight Pct.	Curing Temperature
100	80
100	110
100	130
100	150
100	170
50	80
50	110
50	130
50	150
50	170

2.2.3 Controlling Uniform Mismatch Strain

The deposition of PDMS is a two step process that involves the degasification of the PDMS material prior to spin casting. Degasification is performed prior to spin casting in order to remove excess air bubbles that are created during the mixing of the elastomeric base and cross-linking agent. This step is important because it ensures that the PDMS deposited is free from air bubbles which could result in layers that have defects or are not uniform along the surface. Also, compromising this uniformity would have a negative effect on the residual stress that would need to develop at the elastomer-top film interface in order for the structures to be responsive. Techniques used for degassing include using specially designed vacuum ovens that connect directly to a vacuum pump and can simultaneously degas the material while curing. Since the curing process can be relatively short compared to the degassing process, the solution was fully degassed at ambient temperature to avoid premature curing.

In addition to increasing the modulus, previous studies have shown that PDMS has been found to experience linear shrinkage upon curing [14]. This shrinkage can only occur on the side of the PDMS that is not bonded to the PAA-glass substrate. This causes compressive stresses to form within the layer as shown in Figure 2.4 below. The higher the curing temperature, the more this layer wants to shrink resulting in increased amounts of stress at the bi-layer interface. However, as the curing temperature increases, so does the material's modulus which increases the rigidity of the layer. Essentially, the higher the modulus, the more resistant the material is to conforming. This has a negative impact on the bi-layer structures ability to form particles with small radius of curvatures upon release from the substrate. The results from laboratory tests in this study confirm these assumptions and will be discussed in greater detail in chapter 3.

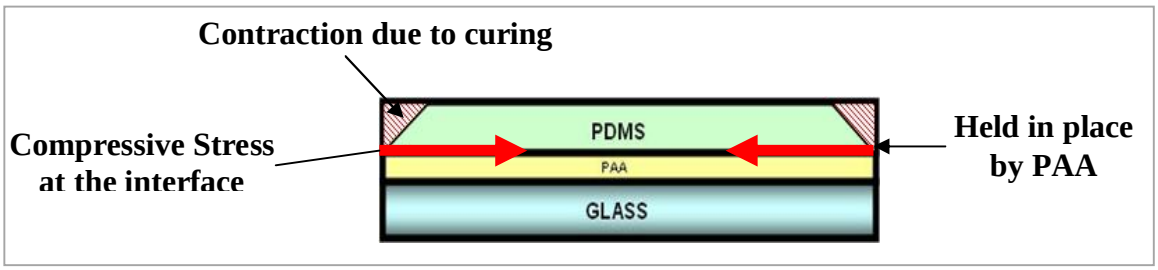

Figure 2.4: Effect of curing on PDMS layer

2.3 Deposition of Top Film Layer

The deposition step in the manufacturing process is dependent upon the material chosen for the top film layer. As discussed prior, four materials were tested in this step: SiC, Parylene-C, Oxidized PDMS and Au/Ti. With the exception of oxidized PDMS, all other options required an alternative deposition process to spin casting. The simplest process involved the oxidation of PDMS to create a thin hydrophilic film layer. This process is performed using a UVO Cleaner ® Model 42 (Jelight Co. Inc.) which performs a photo-sensitized oxidation process that involves the excitation of contaminant

molecules by the absorption of short-wavelength UV radiation [42]. Within minutes of exposure to the UV source, the PDMS material begins to oxidize forming a new ultra-thin layer. In this study, PDMS layers were exposed to UV radiation for 1, 20 and 60 minutes before being tested.

The Unaxis Plasma Enhanced Chemical Vapor Deposition (PECVD) system was used to deposit the thin layers of SiC. The benefits of using this tool were that the film deposition is uniform regardless of the deposition surface and that the system is designed to control the stress of the deposited films. Films such as SiC are, typically, deposited with low stress, but this stress can be adjusted by modifying the ratio of Helium to Nitrogen in the chamber [43]. In this study, SiC layers of 10, 50 and 100 nm were deposited and used for testing.

Figure 2.5: Unaxis PECVD System (courtesy of Georgia Institute of Technology)

A Labcoater PDS 2010 (courtesy of Dr. Peter Hesketh) was used to perform the vapor deposition of Parylene. This vacuum system deposits the material at room temperature and the thickness of the layer can be adjusted by increasing or decreasing the

amount of dimer (in powder from) used in the process. Parylene was deposited at layers thicknesses of 1 and 2 microns.

Two approaches were used for the deposition of the Au film layer. The first is metal sputtering. It is a vapor deposition method where accelerating argon ions hit the surface of a sputtering target consisting of the material being deposited in a vacuumed environment. These ions knock the material off of the target and allow the particles to deposit on the surface of the sample being coated [44].

Figure 2.6: (Left) Gold Sputtering Unit (Right) CVC E-Beam Evaporator (courtesy of Georgia Institute of Technology)

The second approach involved using an electron beam (E-beam) evaporator. E-beam evaporators work using a high-intensity beam of electrons that is focused on the material being deposited. This beam evaporates the material and deposits it on a substrate as a thin layer. The process is usually performed at a low pressure to increase the mean free path of molecules traveling from the evaporation source to the sample being coated. Eventually, e-beam evaporation was chosen as the primary tool used to deposit a metal film layer because, unlike sputtering, it can deposit both Au and Ti which prevents delamination. Also, evaporators only coat the surface facing the depositor as opposed to all exposed sides which could affect the bi-layer structure [45]. In this process, ~5 nm of Ti was deposited as an adhesive layer at 0.1 A/s to bond the Au film to

the elastomeric layer. Au was, then, deposited on top of the Ti. Au was deposited at a thickness of 50 nm. In addition to the Au thickness, the evaporation rate used is also an important processing parameter because it defines the residual stress developed during the deposition. Three deposition rates were used in this study. The Au thickness was 50 nm in all cases.

The processing parameters of each top film material are displayed in Table 2.5 below. Of the film layers deposited and tested, SiC and Au/Ti proved to be the most promising candidates for film layers due to their ability to form responsive particles consistently. These tests were able to show that this approach could be used effectively with both organic and metallic materials as the film layer.

Table 2.5: Processing Parameters of Top Film Layers

Top Film Material	Parameter	Range
Oxidized PDMS	Oxidation Time (min)	1, 20, 60
SiC	Thickness (nm)	10, 50, 100
Parylene C	Thickness (μm)	1, 2
Au/Ti	Deposition Rate (A/s)	1, 2, 3

2.4 Lateral Cutting of the Bi-Layer

Once the materials have been deposited, the bi-layer needs to be cut into small (~1 x 1 mm) rectangular units. One of the key factors in accomplishing the folding of the bi-layer materials into particles is the lateral dimensions of the cuts being made on the bi-layer. The lateral dimensions cannot be so large that the amount of material is too heavy and the residual stress is unable to overcome the material's weight which prevents the bending of the bi-layer structure. Therefore, there is a need to cut the sample into smaller divisions to take full advantage of residual stresses embedded at the bi-layer's interface.

This is perhaps one of the most difficult tasks in this manufacturing process. The difficulty arises from the past methods that were used to create these divisions as well as the need to create smaller divisions in an effort to minimize the size of the particles. The previous method involved manually cutting the sample material with a thin blade either by hand or with a mounted blade on an automated moving stage. Both of these approaches pose problems as far as cutting accuracy, depth of cut, and speed. In addition, there are limitations as to how small the lateral dimensions can be cut since the thickness of the cut is dependent on the razor blade thickness which typically ranges from 200 - 300 um.

In response to this, a rapidly growing technology, laser cutting, has been looked to as a possible alternative. Lasers offer the advantages of a convenient, precise and contamination-free process that chemical means may not offer. Excimer lasers such as KrF (248 nm), ArF (198 nm) and ultra-fast femtosecond lasers are reported as efficient tools for precision micro-structuring of polymer materials. However, many of these lasers have the technical challenges of high capital cost laser equipment, using a toxic gas medium and having slow process speeds [46]. Third harmonic diode-pumped solid state (DPSS) Nd:YAG laser was used to achieve high quality precision engineering of thin polymer films using micro-drilling and micro-cutting by means of direct beam scanning [46]. A laser micro-processing experiment was performed on a thin bi-axially stretched film made of polycaprolactone (PCL) (Mn = 80,000 and density = 1.145 g/cm^3) that was fabricated using a standard solution casting method. The film was drawn to thicknesses ranging from 8-12 um. Another type of film was fabricated through a spin casting method at 500 rpm for 5 minutes. This produced films ranging from 1-2 um. The work

produced acceptable results in that clean, accurate cuts without burning or tearing the layers were produced as seen in Figure 2.7 below. These results can be somewhat misleading since this trial performed cuts through single layered thin films only.

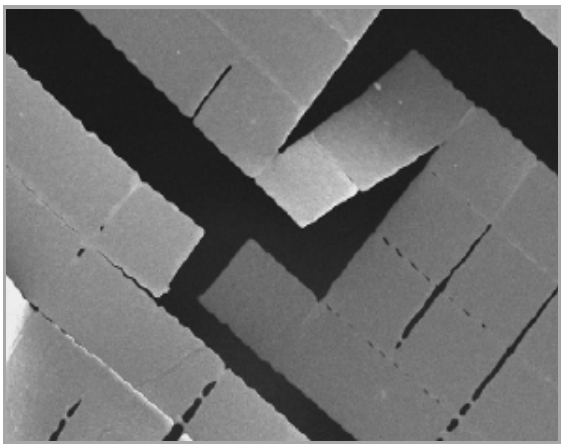

Figure 2.7: Laser-cut thin polymer SEM image [46]

Another study found peeling and cracking to be the common case in bi-layer structures after laser cutting. The main cause of the cracking and peeling was attributed to the mechanical tension due to the differences in substrate and film thermal expansion [47]. In addition to these risks, the high cost of the equipment with respect to the limited amount of usage poses a major concern. This is a technique that will be explored continuously as laser technology becomes more advanced.

On the other hand, with micro-manufacturing growing ever more prevalent, more sophisticated micro cutting tools are finding their way to the market for consumers. Many manufacturers are developing sturdy cutting tools with micro-scale cutting diameters that are available for purchase. It is for this reason that efforts were shifted from laser cutting to developing an automated micro cutting technique to solve this issue.

In the current study, both laser and micro-machining were tested as possible alternatives to the manually-driven cutting method. Laser cutting was performed using

the ULS M-360 CO_2 laser (courtesy of Dr. Samuel Graham). This laser cutting unit offered state-of-the-art positioning system with a motorized X, Y and Z axis and a laser positioning system that can quickly align the laser with the sample being cut. The cutting process was programmed on a computer interface connected to the laser cutting unit. The cutting pattern, speed and laser intensity could be set from this interface. The intensity of the laser could be adjusted from 0-100% to account for the material being cut. The job can be completed within minutes depending on the cut speed settings. Visually, the cut samples seemed neatly cut, but when magnified under a microscope the samples showed signs of burning and tearing along the edges. A second attempt was performed in hopes that a much lower laser intensity or higher cut speed would reduce these effects. The results are summarized in Figure 2.8 showing images obtained using an optical microscope.

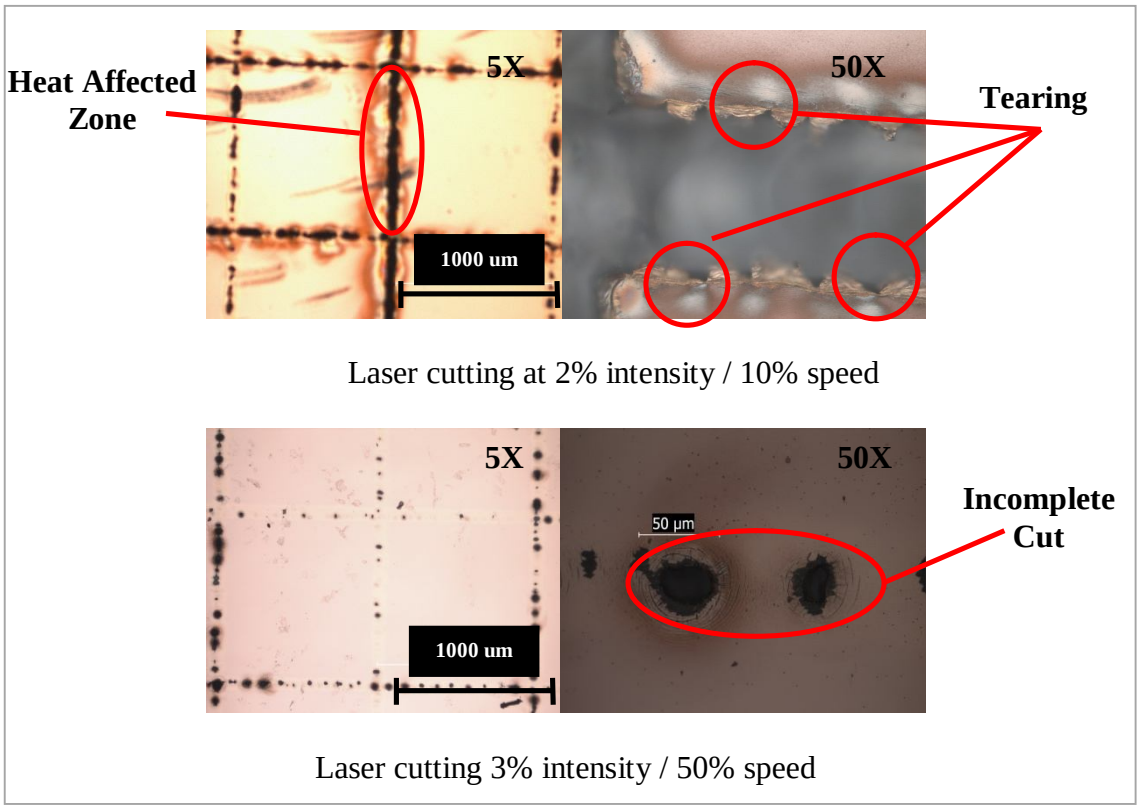

Figure 2.8: Effects of laser cutting

It is clear from the images above that surface tearing and burning still occurs at low laser intensity. Problems were also found when the laser speed was increased to 50%. This adjustment resulted in 'spotty' incisions along the cutting path. Despite being unsuccessful in this trial, it is believed that laser cutting is still a viable option for cutting the bi-layer given the correct laser parameters.

The micro-machining approach offered a cost effective alternative to laser cutting. This process utilizes an automated micro-drilling apparatus. For this process, the bi-layer structure is placed on the cutting surface where it is held in place by two clamps and four screws.

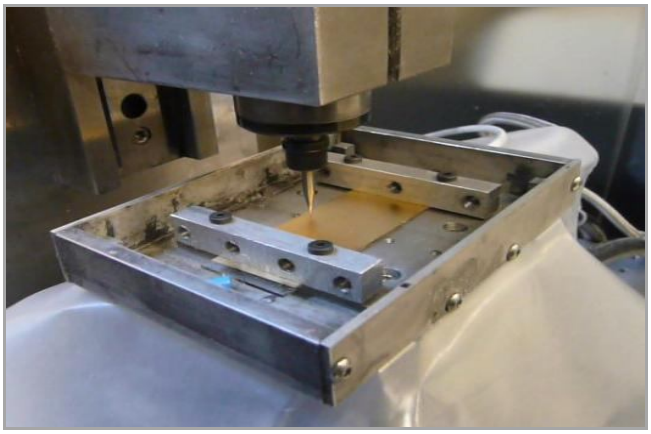

Figure 2.9: Micro-machining cutting surface (courtesy of Dr. Shreyes Melkote)

Initially, it is important to make sure the cutting surface is perfectly leveled and that the sample is positioned flat on the cutting surface to prevent unequal cutting depths along the sample. To verify this, the apparatus consists of a pressure dial that drags along the sample surface to measure the relative flatness. Once the sample is level, the micro cutting tool is placed into the drilling apparatus. The cutting tools used for this task are 2-flute micro end mills (Performance Micro Tool) with cutting diameters that range from 30 um to 150 um. The cutting tool is manually positioned on the work piece with the

assistance of a magnifying scope that helps the user verify the contact distance. A cutting pattern can be programmed into computer software that controls the motorized cutting surface. Since the cutting surface has axes of motion in the x, y and z direction, the depth of cut along with lateral dimensions can be programmed. Once the cutting surface is set and the job programmed, the automated tool switches on rotating the micro-cutting tool at ~60,000 rpm. The results from the work done with this tool were significantly better than the results received from laser cutting.

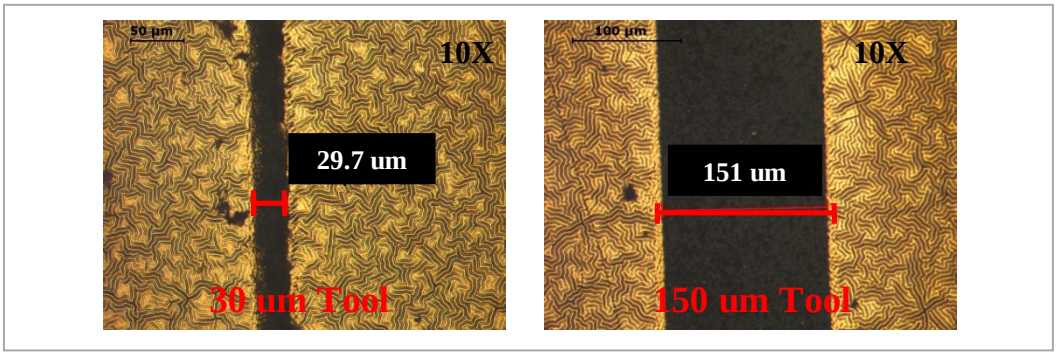

Figure 2.10: Micromachining cutting job with different tool sizes

The images in Figure 2.10 display magnified cutting paths caused by two different micro cutting tools. Unlike the images captured from the laser cutting trials, this approach did not pose the problems of burning or tearing the material in the bi-layer structure. Incisions along the cutting path were neat and consistent across all cutting tool diameters observed. In order to confirm that this approach is suitable for cutting the bi-layer structures, the freshly cut samples would need to be dispersed in water for the final step in the manufacturing process which is the removal of the sacrificial layer, PAA, that will allow the release of the bi-layer and lead to the formation of particles. Upon release, these particles are collected and stored in glass vials containing a viscous glycerol solution that allows the particles to remain dispersed as opposed to floating or sinking in the container, which is the case when water is used as the dispersing medium.

2.5 Triggering the Response

So, how does this process really produce responsive particles? The key to the responsive behavior of the particles is in the curing of the PDMS layer and the deposition of the top film layer during the manufacturing of the bi-layer structure. As discussed earlier, when PDMS is cured, the material shrinks as the solution transforms from a liquid to a solid, but this shrinkage can only occur on the side not attached to the sacrificial layer. Because of this, the bottom end of the PDMS layer is in constant compression. On the other hand, the film layer is deposited on top of the PDMS layer in tension as shown in Figure 2.11.

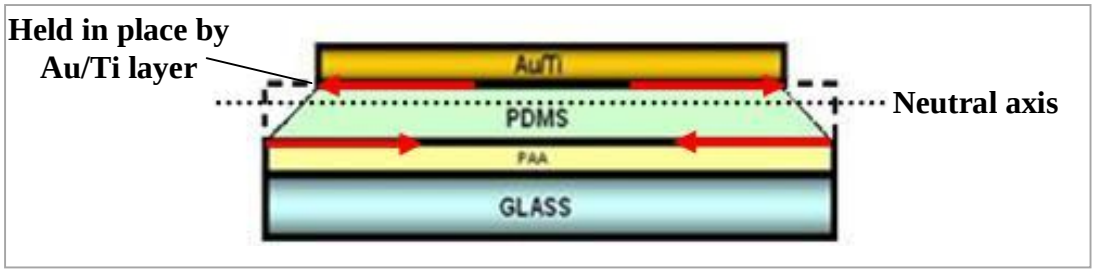

Figure 2.11: Stress within the bi-layer structure

When debonded from the substrate, these stresses are released instantaneously forming free-standing 3-dimensional tubular particles. Upon re-applying the stimulus, heat, the PDMS layer expands to a large extent and the particles return to a 2-dimensional rectangular sheet. When the stimulus is reversed, expansion occurs on the end not bonded to the film layer causing stress to re-develop at the interface of the film and PDMS layer thus leading to re-coiling. This effect is shown in Figure 2.12.

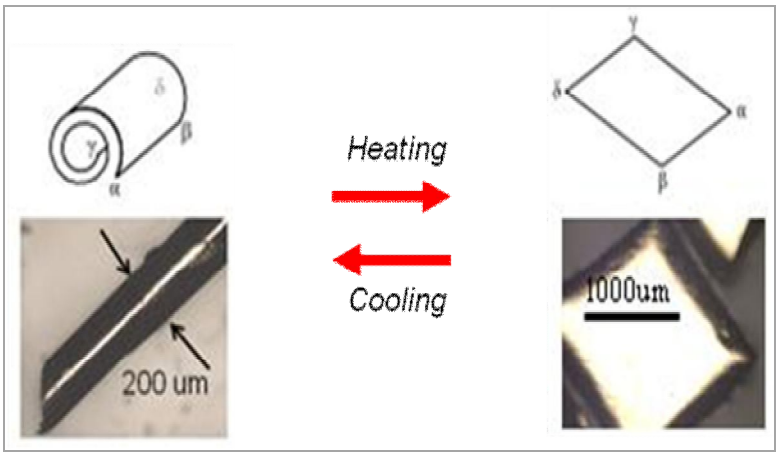

Figure 2.12: Effect of applying/removing stimulus

Temperature is the most widely used stimulus in environmentally responsive polymer systems. The reason this is the case is because temperature is relatively easy to control and is applicable in both in vitro and in vivo processes [48]. This is also the reason temperature was chosen as a starting point for this work. Since this stimulus is already widely explored, an abundance of literature for various experimental set ups and ideas on which to test the bi-layer structure was available. This stimulus was ideal in helping find quick and reliable results.

Temperature is not the only trigger that can be used to cause a change in a polymer system. pH is regularly used to trigger changes in various materials. pH-responsive polymers consist of ionizable pendants that can accept and donate protons in response to the environmental change in pH. As the environmental pH changes, the degree of ionization in the polymer bearing weakly ionizable groups are dramatically altered [48]. Weak polyacids such as polyacrylic acid (PAA) accept protons at low pH and release protons at neutral and high pH [49]. On the other hand, polybases like poly(4-vinylpyridine) is protonated at high pH and positively ionized at neutral and low pH [50]. Knowing this, the proper selection between polyacids and polybases should be

considered for a desired application. Other pH-responsive materials are polymethacrylic acid (PMAA), poly(ethylene amine), poly(L-lysine) and poly(N, N-dimethyl aminoethyl methacylamide).

Recently, responsive materials have been used to create smart responsive surfaces. Smart responsive surfaces are surfaces that have the ability to alter certain characteristics when certain stimuli are applied. In one example, a surface was designed that could alter its wettability by switching reversibly between super-hydrophobicity and super-hydrophilicity through alternative UV irradiation and dark storage [51]. V_2O_5 films were analyzed using X-ray photoelectron spectroscopy (XPS) before and after UV irradiation. Photosensitive inorganic semi-conductor oxides such as TiO_2, ZnO, SnO_2, WO_3, V_2O_5, and Ga_2O_3 are famous for their capability of switching the surface chemical environment between two (oxygen vacancies and hydroxyl) groups [52]. Organic materials usually have a reversible photo-induced transformation between two states. For example, azobenzene, a typical photoresponsive organic material, undergoes a reversible conformational transition between *cis* and *trans* isomers under UV and visible irradiation [52]. It is easy to see that light is becoming more of a common trigger in analyzing these 'smart' structures.

Electrically-responsive surfaces have established some leverage in the last decade. By depositing a low-density carboxylate-terminated self-assembled monolayer on a Au surface, a reversibly switching surface can be fabricated. Electrical potential was used to trigger the conformational transition of the monolayer, resulting in a change in wettability [53]. In addition to these studies, electric and magnetic field responsive polymers have been investigated as a form of hydrogels to have swelling or bending behavior in

response to an external field. It was shown that a polythiophene-based conductive polymer gel actuator could expand and contract in response to an applied potential [54].

Ultimately, wettability of surfaces is dependent on both chemical composition and surface structure. This was proven in a method for reversibly changing between super-hydrophobicity and super-hydrophilicity by biaxially extending and unloading an elastic polyamide film [55]. This approach falls back into the realm of 'strain engineering'. In this approach, the triangular structure film was hydrophobic but was hydrophilic when biaxially extended in both directions. This change was contributed to both the surface tension of water and the average side length change of the triangular structure upon biaxial extension and unloading [55]. Matrix surfaces, similar to the ones developed by one research group which include polymer, silica, and metals could be functionalized with stimuli-responsive polymers to produce highly responsive interfaces between solid and liquid (mostly water) phases. The property of the modified interface can give a dynamic on-off system by changing the hydrophobic/hydrophilic surface function and the pore size of porous membranes [48].

In addition to all of the triggers discussed, more sophisticated triggering systems are arising. For example, glucose responsive polymer systems have been investigated due to its biomedical market potential [48]. Glucose responsive hydrogel systems can provide self-regulating insulin release in response to the concentration of glucose in the blood. This, in turn, regulates the concentration of insulin within a normal range [48]. Also, dual- and multi-responsive surfaces have been fabricated and found greater applicability in drug delivery since many areas of the body differ in temperature and pH environments.

CHAPTER 3

CHARACTERIZATION OF RESPONSIVE PARTICLES

These three-dimensional particles are characterized in terms of the radius of curvature because of their tendency to take the form of a scroll or coil-shaped object. It is known that the size of the radius of curvature is highly dependent on the amount of residual stress that develops at the interface of the bi-layer structure, but many factors contribute to this. Many of these factors are expressed in the theoretical equation that was developed during experimental research on stress measurement in thin films bonded to substrates [7, 17, 19]. In this study, three of the factors that contribute to the radius of curvature will be analyzed. The first is the thickness of each layer in the bi-layer structure. The second is the modulus of the each layer. The final and perhaps most important is the uniform mismatch strain generated between the two materials in the bi-layer structure. This mismatch strain is caused by lattice mismatch that can be attributed to a difference in the material properties of the two materials. In this case, the difference in thermal expansion of the layers is the primary reason. It is also this reason that temperature is the appropriate stimulus for these responsive particles in order to take advantage of this property difference.

3.1 Characterization Tools & Methods

In research, there is usually a variety of useful apparatus and approaches for collecting certain information and characteristics about a specimen being analyzed. In many cases, it is usually left up to the researcher to use experience or the available literature around to decide which apparatus or approach is the most efficient, fastest, cheapest or most reliable. Thus, there is a need to prove why the methods that are being

used to collect the data are the best possible methods. In this section, relevant literature that outlines the advantages and disadvantages of some of the common methods and apparatus used to collect the data that allow the characterization of the responsive particles will be discussed. From there, results from using these characterization tools will be examined.

3.1.1 Characterization of Modulus

Measuring the modulus of the PDMS thin layers is an important part of the mechanical analysis of the bi-layer structure. It is important to know the Young's modulus of PDMS in order to use Eq. 4 presented in chapter 1. Various characterization techniques such as tensile tests, electrostatic pull-in tests, membrane-bulge tests, beam-bending tests, micro-bridge tests, frequency-response tests and indention tests have been widely developed to extract Young' modulus [31, 56-59]. In this study, dynamic mechanical analysis (DMA) was used to accurately determine the elastomeric material's mechanical properties.

In previous studies, the Young's modulus of PDMS has been found to fall between 0.1 - 3 MPa depending on the preparation conditions of the material [40]. In this study, Young's modulus was measured as a function of curing temperature using thin slabs of PDMS. After curing, the slabs were removed from the mold and stored for at ambient conditions for an additional 24 hours before testing. The dimensions of each PDMS slab were 25.4 mm x 50.8 mm x 1.5 mm. Five samples were cut from each slab into 20 mm x 8 mm x 1.5 mm tensile specimens and tested using a DMA Q800 (TA instruments. To make measurements, each test specimen was mounted on tensile clamps. These clamps were tightened using a torque screwdriver that was set to ~3 in-lb to ensure

that all specimens were tested under the same conditions. The unit was programmed to run a strain ramp test that applied strain to each sample at a rate of 1%/min up to 25% strain. Data from these tests were presented in the form of a stress-strain curve and the Young's modulus was calculated as the slope of the linear regime.

3.1.2 Characterization of Thickness

The profilometer used in this study was a non-contact optical profilometer (Zygo Corp.) that uses the phase change of light reflecting from various heights of similar materials to measure the uniformity of a flat surface or the horizontal distance between two adjacent surfaces. A pre-made step had to be created with a thin blade or by placing tape or another glass slide on part of the sample during deposition and curing in order for the profilometer to be able to read the change in thickness between the substrate and the layer(s). The objective of this apparatus was to measure thicknesses from 500 nm to 10 microns. Luckily, many profilometers today are able to measure surfaces thicknesses as thin as 20 nm before they begin to lose sensitivity.

In making the samples for the thickness measurements, PDMS was deposited directly on a glass substrate without depositing the sacrificial layer. Three sets of PDMS solution were prepared at 100% (i.e. pure PDMS), 70% and 50% by weight concentration to Hexane. Next, each solution base was poured on a glass substrate and spin cast for 3 minutes at various spin rates. The spin cast samples were cured at 110 °C for 20 minutes. In addition, a scanning election microscope (Hitachi 3500H SEM) was used to confirm the data attained by the profilometer.

3.1.3 Characterization of the Radius of Curvature

An optical microscope, the Leica DFC420 (Leica Microsystems), was used to observe the resulting radius of curvature of the particles created from the tests described above. This tool provides high-resolution color and monochromatic images as well as image analysis software to measure the diameter and radius of curvature of the particles in this study.

For this analysis, particles were placed on thin glass slides and viewed at various magnifications ranging from 5x to 50x. For each trial, multiple particles manufactured under the same processing parameters were examined. Average values were calculated along with the standard deviation of the values obtained. This method was used to observe the effects of changing the modulus and thickness parameters in the bi-layer.

3.2 Results of Modulus Characterization

After obtaining the modulus of the PDMS at various curing temperatures, a second set of test specimens were prepared to investigate the effect of diluting PDMS on the modulus. Prior to curing, each solution of PDMS was mixed with 50% Hexane by weight percentage. Table 3.1 below displays the results from this both sets of tests performed. As expected, diluting the PDMS solution resulted in a much weaker material. This can be attributed to the fact that the solvent used to dilute the PDMS causes the polymer chains to swell instead of interacting with each other to form tight bonds like they normally would in a concentrated solution.

Table 3.1: Effect of curing temperature on PDMS modulus

Curing Temperature	Average Modulus (100% PDMS)	Average Modulus (50% PDMS)
80	1.13 +/- 0.07	0.93 +/- 0.06
110	1.82 +/- 0.17	1.11 +/- 0.04
130	1.93 +/- 0.05	1.3 +/- 0.05
150	2.12 +/- 0.06	1.57 +/- 0.08
170	2.23 +/- 0.07	1.71 +/- 0.07

With the approximate modulus of the elastomeric layer known at each temperature, the bi-layer structures could now be manufactured to show how altering the modulus affects the size of the particles produced. As with the modulus testing, two batches of PDMS solution (100% and 50% PDMS) was prepared prior to manufacturing the bi-layer structures. Each structure was built using the same parameters for spin casting the PDMS layer and film layer deposition. The only step that was altered for each sample was the curing temperature of the elastomer. After the bi-layer structures were cut and the sacrificial layer dissolved away, the resulting particles were acquired and stored in separate vials. Next, several particles from each vial were examined using an optical microscope to measure the diameter of the particles. Table 3.2 below displays the results from that analysis.

Table 3.2: Effect of modulus on particle diameter

% PDMS	Curing Temperature	Average Modulus (MPa)	Particle Diameter (μm)
100	80	1.13 +/- 0.04	257.2 +/- 14.3
	110	1.82 +/- 0.09	234.4 +/- 8.2
	130	1.93 +/- 0.03	221.2 +/- 9.1
	150	2.12 +/- 0.03	251.3 +/- 17.9
	170	2.23 +/- 0.04	253.2 +/- 11.8
50	80	0.93 +/- 0.03	275.5 +/- 26.2
	110	1.11 +/- 0.02	168.1 +/- 6.3
	130	1.3 +/- 0.03	163.7 +/- 8.4
	150	1.57 +/- 0.04	187.9 +/- 9.2
	170	1.71 +/- 0.04	192.5 +/- 11.5

Based on the data collected from the tests, the particle diameter seems to change significantly as the modulus of the elastomeric layer is altered, but it is still unclear whether or not increasing the modulus promotes smaller or larger particle diameters since in both cases it does both. On the other hand, it can be seen that diluting the PDMS solution has a positive effect on the particle diameter in producing smaller diameters (with the exception of 80 °C). This effect may have more to do with the diluted solution producing much thinner layers than the undiluted solution rather than the difference in modulus. Therefore, additional testing must be performed on the other factors that affect the particle diameter in addition to the modulus. In the next study, the thickness of the PDMS layer was analyzed in hopes of gaining a better understanding of the mechanical properties of the particles.

3.3 Results of Thickness Characterization

Thickness measurements were taken from test specimens for each PDMS solution and spin rate. Table 3.3 displays the data collected from the profilometer. In addition, the Hitachi 3500H SEM was used to confirm the thickness measurements data attained

by the profilometer and is shown in Figure 3.1. It is clear from the results that both diluting and increasing the spin rate during deposition decrease the thickness of the PDMS layer. This could very well explain why the diluted PDMS material used during the modulus testing produced smaller particles despite having modulus values similar to that of the undiluted samples. Both modulus and layer thickness are two important factors outlined in the theoretical equation used to characterize these particles, but there are other factors that need to be addressed in this study.

Table 3.3: PDMS layer profilometer data

% PDMS	**3000 rpm (µm)**	**4000 rpm (µm)**	**5000 rpm (µm)**
100	11.5 +/- 0.5	9.71 +/- 0.3	7.39 +/- 0.4
70	9.33 +/- 0.3	7.9 +/- 0.4	5.86 +/- 0.2
50	7.2 +/- 0.2	6.8 +/- 0.1	4.45 +/- 0.2

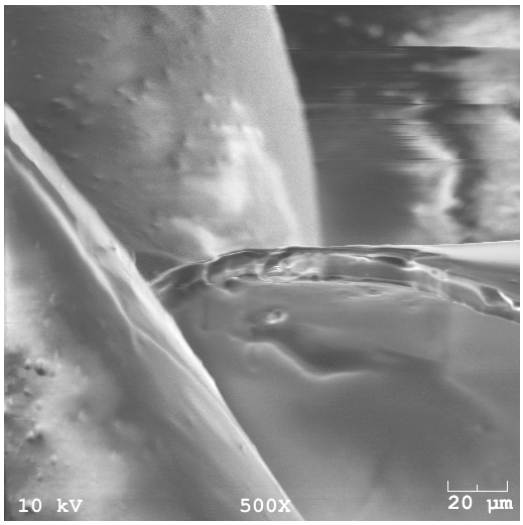

Figure 3.1: Particle thickness SEM image

3.4 Results of the Radius of Curvature Characterization

Based on Eq. 4, there are three factors that have an effect on the radius of curvature of the particles. Of these factors, the amount of residual strain at the interface

of the bi-layer is the only parameter that cannot be found directly. Instead, this parameter can be found indirectly by obtaining the radius of curvature experimentally and, then, solving for the strain in Eq. 4.

According to the experimental results discussed earlier, curing temperature plays a large role in the size of the particle. This makes sense because as the curing temperature increases, the PDMS layer wants to shrink more upon cooling meaning more residual stress has the opportunity to develop at the interface. However, as the curing temperature increases, so does the modulus of the PDMS which leads to a more rigid bi-layer that is difficult to fold, thus, resulting in looser particles. This is confirmed by combining the data in the three previous characterization studies in Figure 3.2 below.

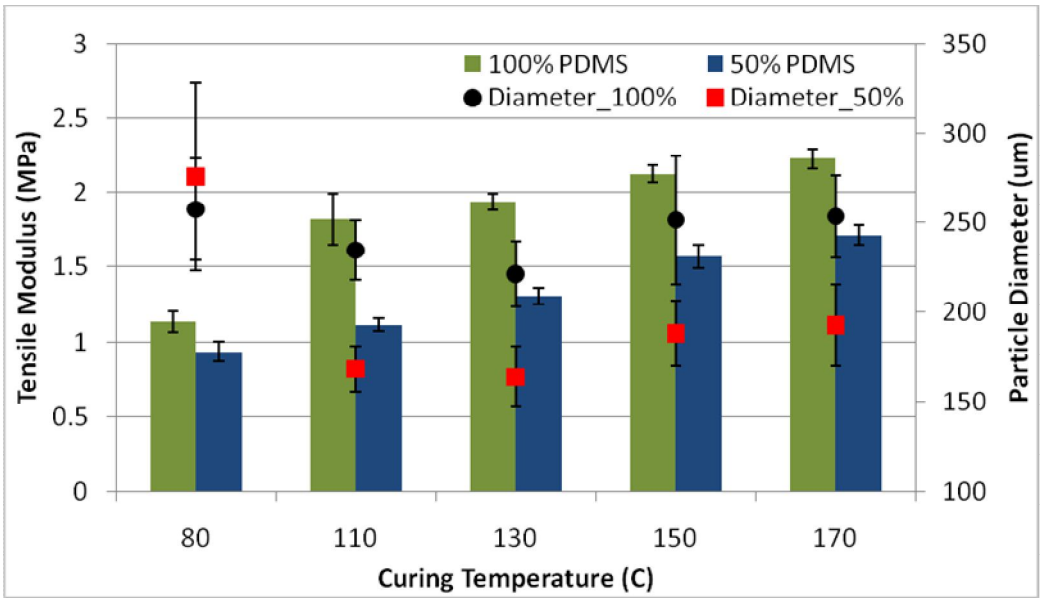

Figure 3.2: Effect of curing temperature on PDMS modulus & particle size

Figure 3.2 suggests that there is an optimum curing temperature in which the bi-layer structures should be manufactured in order to achieve the smallest possible radius of curvature. Using Figure 3.2 and Eq. 4, the interfacial stress can be indirectly

calculated since all other values are now known. In Table 3.4 the interfacial stress as a result of the process parameters and materials chosen is calculated.

Table 3.4: Effect of processing parameters on interfacial strain

% PDMS	T_{cure}	Thickness Ratio (h_f/h_s) [μm]	Modulus Ratio (m) [Pa]	Radius of Curvature (ρ) [μm]	Interfacial Strain (ε)
100	80	.005	64791.4	128.5	0.052155
	110	.005	40212.9	117	0.057265
	130	.005	37791.27	111	0.060361
	150	.005	34453.78	126	0.053176
	170	.005	32831.52	127	0.052758
50	80	.01	78432.67	138	0.024753
	110	.01	65741.65	84	0.040544
	130	.01	56131.58	82	0.041438
	150	.01	46722.58	94	0.036069
	170	.01	42723.76	96	0.035285

The data presented above gives a clear idea of the importance of the processing parameters of the elastomeric layer in the size of the resulting particles, yet there is nothing that provides insight into the how the processing parameters of the top film layer effects the particles.

3.5 Au/Ti Film Deposition Rate

As discussed earlier, the residual stress developed at the PDMS/Au interface is a combined result of the PDMS tendency to shrink and the fact that Au is deposited in tension during E-beam evaporation. In order to provide some idea as to how the deposition of the top film layer affects the final state of the particles produced in the process, a series of tests were performed using the process for depositing the Au/Ti layer. The deposition rate of the Au film on the surface of the PDMS layer and the Au film thickness are essential to the residual stress developed at the bi-layer interface. Bending is highly dependent on the difference in thermal expansion rates and modulus between

the film and PDMS. Also, the reversible response of the particles is dependent on how well the film is adhered to the PDMS layer as well as the ductility and fatigue strength of the film layer. It is known from the analysis covered on the bi-layer structure that the top film layer is deposited in tension, but this is assumed to be primarily controlled by the elastomeric layer in which it is deposited on. On the other hand, changing the rate at which the Au is deposited might have an effect on how much stress develops at the interface of the top film layer and the elastomeric layer.

To test this hypothesis, multiple samples of bi-layer structures were manufactured simultaneously using the same PDMS solution, spin casting parameters and curing parameters. Next, samples were divided, labeled and subjected to an e-beam evaporation process for the deposition of the Ti and Au layers. For every sample created, a 5 nm Ti adhesive layer was deposited at 0.1 A/s. For the first set of samples, 50 nm of Au was deposited at 1 A/s. The second set was deposited with 50 nm of Au at 2 A/s. The final set of samples was deposited with 50 nm of Au at 3 A/s. Once the bi-layer structures were built, each sample was cut and the sacrificial layer was dissolved. The particles were collected and examined using the optical microscope. Figure 3.3 displays the results of this examination.

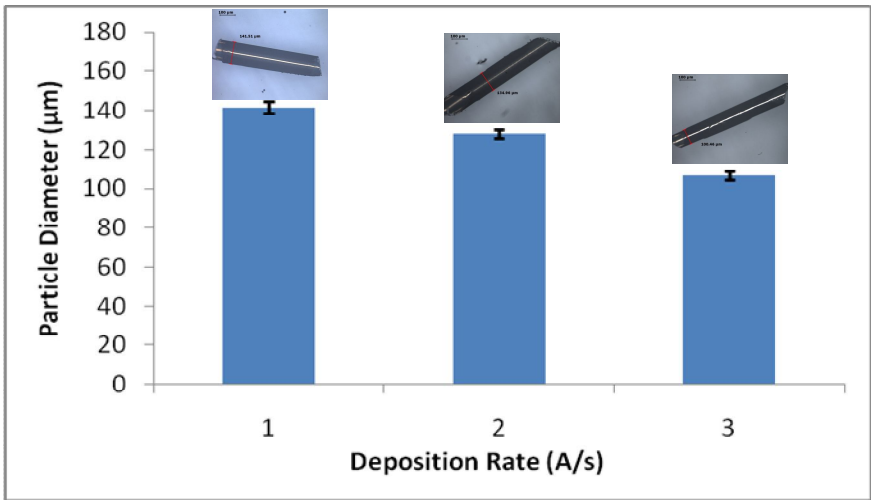

Figure 3.3: Au/Ti deposition rate vs particle diameter

For the previous experiments, the film layer was always deposited 1 A/s which was the default deposition rate setting for Au. As the rate of deposition increased, the resulting particle diameter decreased in a linear fashion. At the highest deposition rate tested, particles sizes averaged ~100 microns in diameter which is much smaller than the particles achieved in the previous tests where only PDMS was altered. The decrease in diameter can be attributed to the additional stresses created in the bi-layer as the molecules travel in the low pressure chamber and collide with the elastomeric surface. As the deposition rate is increased, more Au atoms are hitting the surface per second and do not allow as much relaxation of the stresses at the interface to occur. This results in the development of more stress at the interface. It should also be noted that temperature could also be affected by the increase in deposition speed. As the deposition speed is increased, the temperature inside the unit might also increase, but this was not measured.

3.6 Material System Evaluation

As discussed, the bi-layer is composed of an elastomeric material, PDMS, and a top film layer. Of the four materials tested as possible film layer candidates, Au and SiC

were the only materials that consistently formed particles. The other materials, parylene-C and oxidized PDMS, were not effective because they lacked at least one essential quality for a good film layer. For example, parylene showed signs of delaminating when the structure was released from the substrate. Without the ability to remain bonded to the elastomer, the film could not sustain the development and release of residual stress. On the other hand, the oxidation of PDMS through UV radiation was only temporarily, eventually resulting in the material reverting back from hydrophilic to hydrophobic. In manufacturing and characterizing the two material systems chosen, key differences were found in how these structures responded to the same stimulus. Many of these differences can be directly attributed to certain material properties found in the top film layer.

It is important to note that the properties of the responsive bi-layer structure change depending on the material system that the structure is built upon. In this analysis, two materials systems were studied in terms of their response. The first was manufactured using Au film with a Ti adhesive layer, while the second set was manufactured using SiC as the top film layer. The elastomeric portion of the bi-layer was manufactured identically in terms of curing temperature, curing time and spin casting parameters, but according to Figure 3.4, it is clear that two very different types of responsive particles resulted. The bi-layer structure consisting of the Au/Ti film layer formed tight, organized scrolls, while the bi-layer structure consisting of the SiC film layer produced very loose, unorganized coils.

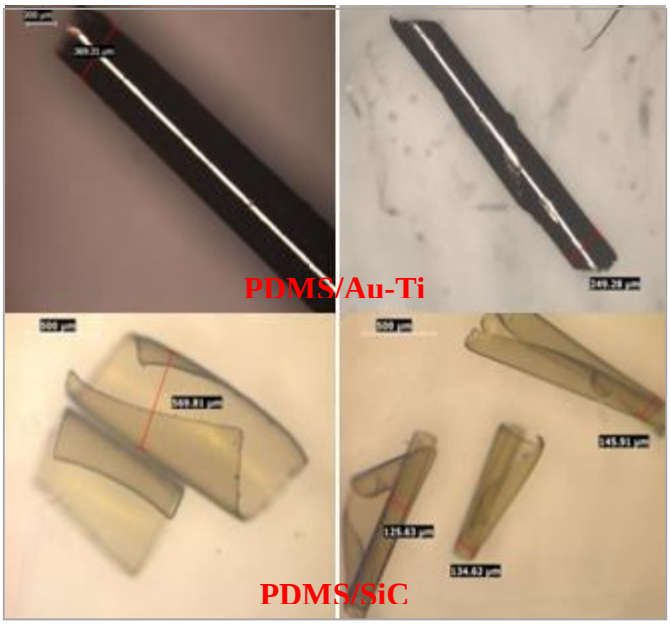

Figure 3.4: Comparing particles for two material systems

Both films have coefficients of thermal expansion that are far different from PDMS, so the question herein lies, “Why did they not provide similar results?” The primary reason relates back to Eq. 4. In Table 3.4, it can be seen that SiC has a smaller coefficient of thermal expansion than Au, therefore it would seem that the difference in thermal expansion in that material system would be greater and would allow more residual stress to develop than what would be found in PDMS/Au when the stimulus is applied. This may be true, but there is an important factor that should not be overlooked. One of the main factors that contribute to the radius of curvature outlined in Eq. 4 is the modulus of the respective layers. As mentioned previously, these factors are in a constant struggle to control how the material system will respond when released from the substrate. As Table 3.5 shows, the SiC film has a much higher modulus than the Au/Ti layer meaning the SiC film is much stiffer and requires more residual stress to fold. Despite having the same thickness and greater difference in thermal expansion from

PDMS, the stress at the interface is not enough to form a scroll with a small radius of curvature. Instead, half ring and slightly curved arcs of large radius of curvature result.

Table 3.5: Property comparison between top film layer materials

Material	**Coefficient of Thermal Expansion (α) [K^{-1}]**	**Layer Thickness [nm]**	**Young's Modulus [MPa]**
PDMS	960 x 10-6	10,000	0.1 – 3
Au	14 x 10-6	50	78
SiC	3 x 10-6	50	410

CHAPTER 4

DEMONSTRATION OF THE REVERSIBLE RESPONSIVE PARTICLE BEHAVIOR

It has been shown how strain engineering can be used to manufacture polymer particles by building a bi-layer consisting of PDMS coated with a thin layer of Au/Ti or SiC. In addition, techniques for characterizing the particles were discussed and were able to show how the diameter and length of the resulting particles could be tuned by carefully choosing the appropriate processing parameters during the manufacturing process. The next step is to demonstrate that these particles can actually respond when a stimulus is applied. In referring back to Figure 2.12, it was shown that these particles possess the ability to change its geometry from a two dimensional flat sheet to a three dimensional cylindrical particle. Because of this geometry change, many other properties are also altered. To show this effect, experiments were devised that recorded changes in properties as a result of the change in geometry of the responsive particles. Each approach needed to capture these property changes as the stimulus was applied and removed. This was achieved through rheology and light absorption testing. Additionally, an application which takes into account the ability of the particles to alter its geometry upon demand was examined. This application involves the selective capturing, transport and controlled release of another substance which tests the particles ability to be used as a delivery vehicle.

4.1 Viscosity Change of Particle Solution

A viscometer, the DV-I Prime Digital Viscometer (Brookfield), was used to measure the change in viscosity as heat was applied via hot plate to a solution containing

responsive particles. The cylindrical shape of these tiny objects allows the unique ability of the particles to flow along a fluid flow field. Due to this distinctive quality, the particles add little resistance to the fluid in which it is dispersed. The purpose of this experiment was to show that the opening of the particles, upon being placed in a heated solution, would result in a sudden increase in resistance and thus, viscosity.

A key decision was the choosing of an appropriate solution in which to perform this test. There were a number of possible options to choose from. The cheapest option considered was water. One of the reasons water is not a good medium for this test is that the particles tend to respond in temperatures closer to the boiling point of water. This means that water is already in the process of evaporating before any measureable results can be obtained. Another option was to consider the fluid used to store the particles, glycerol. Since glycerol is hygroscopic in nature, the solution sometimes contains a certain percentage of water. It is because of this reason that this option might pose some of the same issues at temperatures above 100 °C. Eventually, silicon oil, a fluid very similar to PDMS in nature was chosen. The benefits of Si oil include the fact that it does not degrade at high temperatures and the viscosity of the fluid changes linearly with respect to temperature.

Two tests were performed in this experiment. In each test, two heating and cooling cycles were performed. The first test was performed on silicon oil with no dispersed particles. The second test was performed on the solution containing several dispersed particles. Figure 4.1 shows the change in viscosity of the silicon oil without dispersed particles for two heating and cooling cycles. This model gives a clear picture of the behavior of the fluid medium as the temperature is increased and decreased.

Figure 4.2 shows the viscosity change of the same fluid medium with the addition of the responsive particles for two heating and cooling cycles.

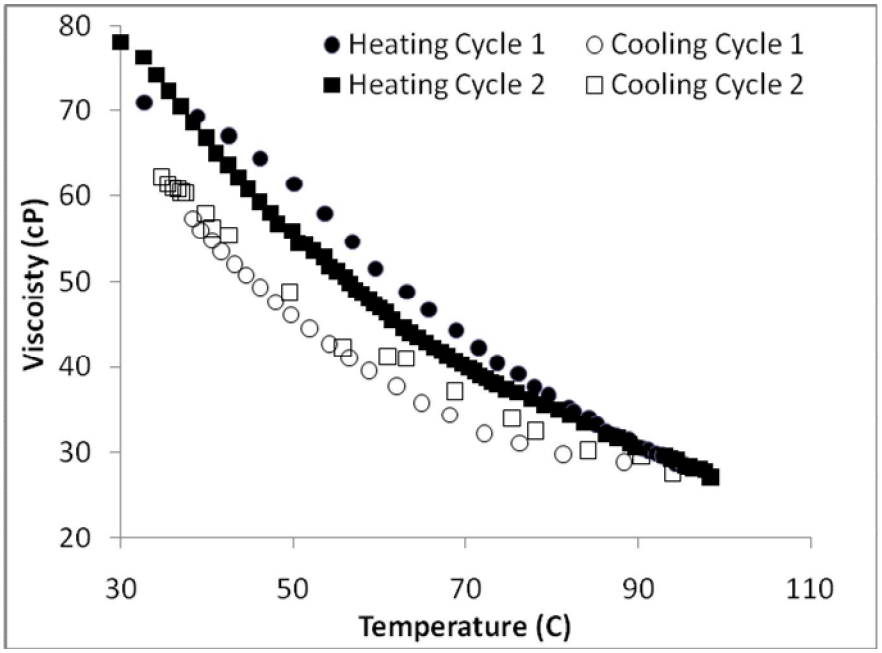

Figure 4.1: Viscosity of Si oil

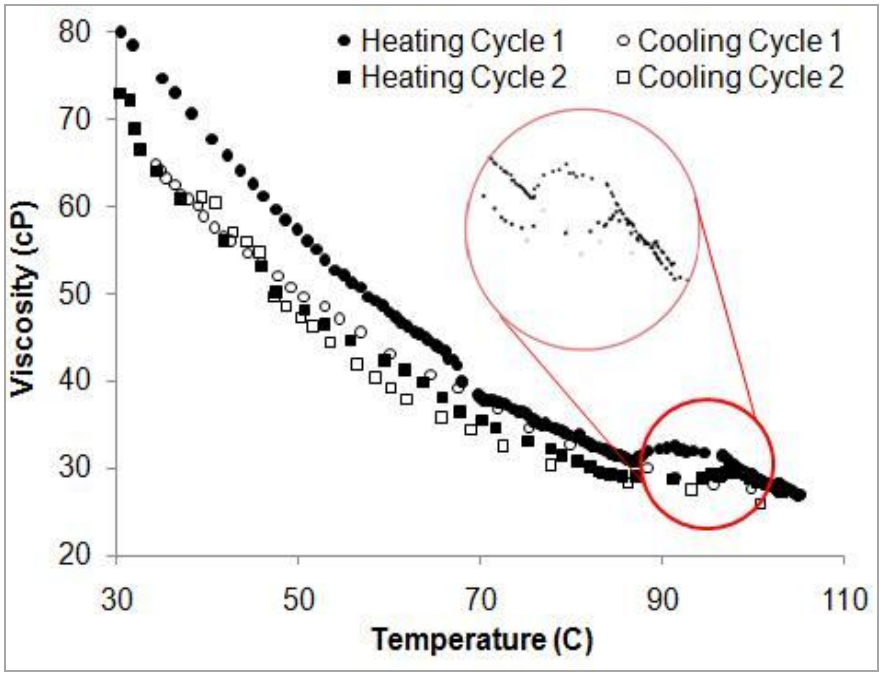

Figure 4.2: Viscosity of Si oil with particles

In comparing the two figures, it can be seen how the addition of particles affect the viscosity of the fluid. Figure 4.1 shows a viscosity reading that is fairly uniform, while Figure 4.2 shows a small viscosity rise as the particles begin to open at high temperatures. The opening and closing of the particles are confirmed visually and through the rheological data presented in the above figures. This experiment displayed promising results and will be extended to track the response of other particles made from different material systems.

4.2 Light Absorption Change of Particles

An Axio Observer Inverted Tissue Culture Microscope (Carl Zeiss) was used to measure the change in light intensity between responsive particles in the closed, tubular stage and the opened, flat stage. Densitometric analysis was performed on images of responsive particles in both the open and closed stage using image analysis software. Densitometry measures of optical density of light-sensitive materials. The optical density is measured by light absorption through an object. This is achieved by taking the average grey value of the pixels that comprise each monochromatic image recorded by the microscope. These values are based on a scale created from a light intensity histogram [60]. The idea is that when the particles are opened, additional light will be absorbed.

For this experiment, the responsive particles were observed using the optical microscope. Ten images of the responsive particles were recorded. Five images were recorded while the particles were in the closed, tubular phase, while five more images were taken of the same particles in the opened, flat phase. Figure 4.3 displays these images.

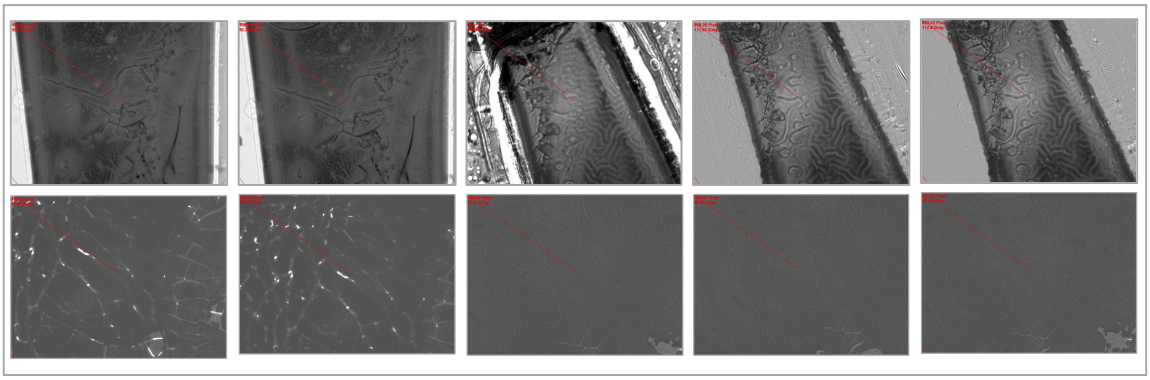

Figure 4.3: Light Intensity Images

By observing the images in Figure 4.3, it is clear that less light is able to transmit through the opened particles, but this needs to be verified using the image analysis tool. The densitometic mean tool recorded the light intensity on a scale from 0 to 4095. The value of 4095 signified pure white light while 0 was the value established for black or the absence of light. According to the tool used to evaluate the light intensity of these images, the light intensity dropped by approximately 17% during the transition from a cylindrical particle to a flat sheet. This means that an addition 17% of light is absorbed when the particles are in their open, flat phase than in the closed, tubular phase. The densitometric mean values were recorded in Table 4.1 below.

Table 4.1: Densitometric Mean Values

	1	**2**	**3**	**4**	**5**	**Average**	**Standard Deviation**
Open	86.47	87.81	87.44	87.01	86.88	87.1	0.52
Closed	92.31	92.12	117.7	117.8	106.8	105.3	12.79
% Difference	--	--	--	--	--	0.17	--

4.3 Capture/Release Ability of Thermo-Responsive Particles

After proving the reversibility of the responsive particles, there was a need to apply the particles to a novel application that utilizes that particles ability change its geometry on command. There are a number of potential applications in which this response can be applied to. In one application, the particles could be used as a carrier of biomolecular substances that the body needs or medications that could be used to treat illness. Many studies in drug delivery systems were performed previously, and significant progress had been made in the design and synthesis of stimuli-responsive polymer capsules used for controlled drug release, ranging in the size from nanometers to microns [5, 33, 61]. In order for the particles to achieve such a feat they would have to exhibit the ability to selectively capture, transport and release a material upon command. It is believed that the qualities of these particles which include the ability to reversibly alter their geometry, a large exposed surface when opened flat, and the ability of the particles to travel in a flow field when they are in their closed, tubular state makes them suitable candidates for this application.

In order to prove that the responsive particles can be used as a delivery vehicle, an experiment involving fluorescent isothiocyanate-terminated poly(ethylene glycol) (PEG-FITC, Nanocs) was used. PEG-FITC was used because the polymer can be absorbed by Au which served as the top film layer material for the particles used in this experiment. In this study, the particles were exposed to PEG-FITC in both their open and closed state. For closed particle exposure, the bi-layer structure was manufactured and released to produce particles. Next, the particles were exposed to PEG-FITC solution in a glass vial for two hours. The particles were, then, rinsed several times by water and examined

using a fluorescent microscope. For open particle exposure, the bi-layer structure was exposed to the PEG-FITC solution prior to the cutting and releasing step to ensure that the PEG-FITC was completely absorbed across the Au layer. Next, the samples were cut and released to produce particles. The particles were placed in a solution bath and the temperature was elevated in order to open the scrolls.

Fluorescence microscope images were recorded at 4x magnification with a DMLB Microscope (Leica Microsystems, Inc.) and an Orca-ER fluorescence imaging camera (Hamamatsu Photonics, K.K.) with the appropriate FITC light source and filter (for 495 nm excitation and 521 nm excitation, respectively). Image acquisition and presentation was facilitated by SimplePCI 6 (Hamamtsu Corp.) and Adobe Photoshop CS4 (Adobe Systems, Inc.) software. In examining the absorption of the particles exposed in their closed state, it was noticed that the PEG was unable to diffuse into confined regions of the tubular particle. This is verified in Figure 4.4 below.

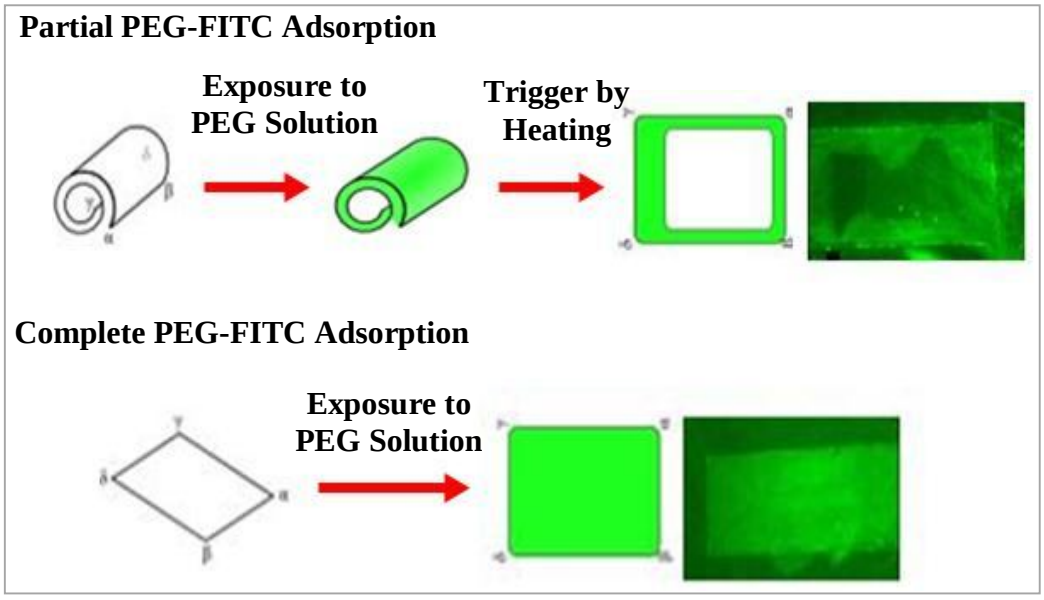

Figure 4.4: Partial/Complete PEG-FITC absorption

For the final stage of the experiment, the entire process of capturing, transporting and releasing was examined. First, cleaned particles were opened by placing the particles in a heated solution. Once opened, the particles are transferred to a PEG-FITC solution where they are exposed. Upon cooling, the particles reverted back to their cylindrical shape. While in the closed state, these particles are able to align and follow linear and circular flow fields, as was shown in the previous rheological study, which allow for easy transport in fluid mediums. Next, the particles were removed from the fluid medium and moved to another heated solution to be re-opened. When the particles are opened for the second time they are moved to a beaker of hot water where they were allowed to float freely for an hour allowing desorption of the PEG-FITC to occur in the water. Upon re-examination of the films using the fluorescent microscope, it is confirmed that the entire PEG-FITC was removed.

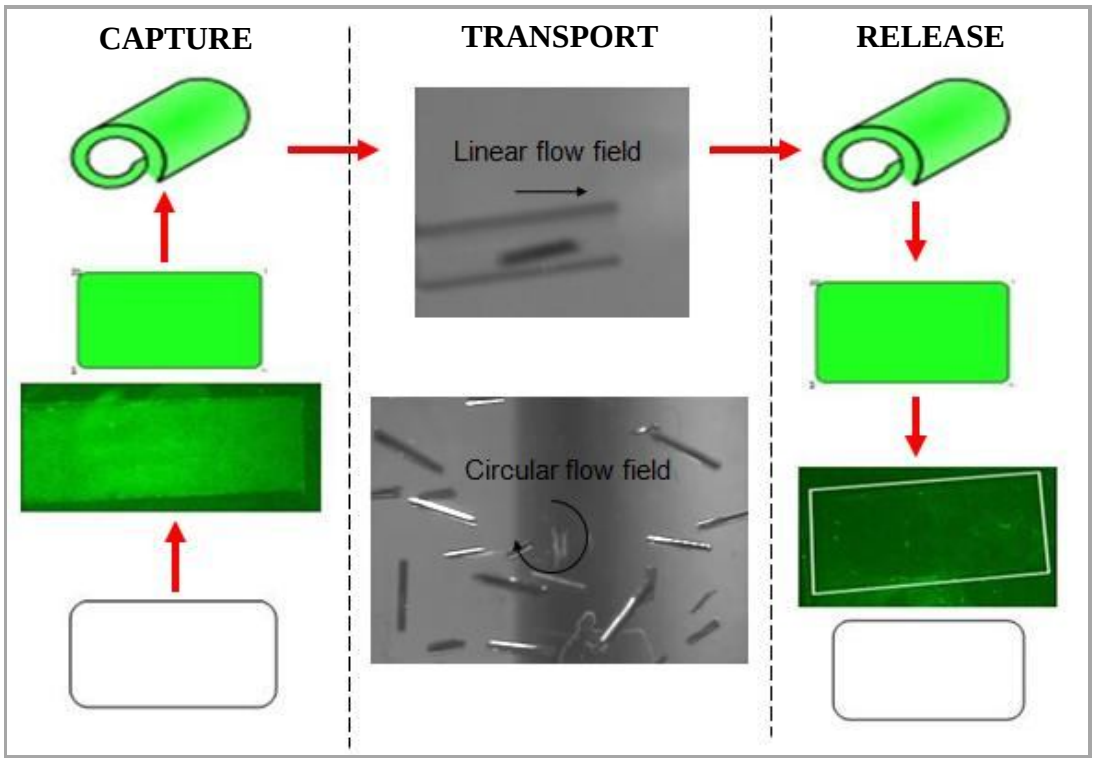

Figure 4.5: Capture/Release ability of responsive particles

This experiment provided significant evidence that these particles could be used for a novel application that utilizes the responsive particles' ability to reversibly alter its geometry. In addition to being utilized in the biomedical field as described earlier, the qualities exhibited by the particles in this study can be used as a filtering mechanism that selectively absorbs contaminants before being removed or filtered from a solution.

CHAPTER 5

LARGE-SCALE MANUFACTURING OF RESPONSIVE PARTICLES

It was demonstrated in the previous chapters that responsive particles could be made in a simple, repeatable and cost effective manner using strain engineering. By studying the processing conditions one can focus on how to develop new approaches for manufacturing. Engineering design tools were used to explore the manufacturing method of the responsive particles to see how they could be used to improve the current process and processes like this one by presenting a new large-scale approach that is low-cost, high in quality, and provides improved efficiency in the manufacturing process. The focus of this chapter will be to propose such an approach for the mass production of the particles by scaling up the manufacturing process discussed in this thesis.

The manufacturing approach used to create these responsive polymer-based particles are based on the efforts began by previous research groups [13, 17, 28, 62, 63]. Prior work on responsive particles included the manufacturing of polymer particles that could alter their geometry, flow characteristics and adsorption properties upon the stimulation of an environmental change which gave them great potential as components in smart composites and as drug delivery systems [17]. This study addressed the material selection, manufacturing, and characterization processes for advanced polymeric materials that were in practice at the time. Now, in order to understand how to plan for the mass production of such particles, the same must be done. Each of the tasks within the manufacturing process needs to be analyzed and understood. Next, a subset of principles to test and improve needs to be selected. Once aspects of the process have been clarified and evaluated, an improved concept solution can be displayed. Various aspects

of these processes will be optimized such as cost, production time, quality, and safety to ensure that multi-layered polymer composites that are affordable and reliable can be produced.

Several engineering design tools based on the ideas of the Pahl and Beitz approach to engineering design principles were chosen to be implemented. Currently the manufacturing of the responsive particles is on a laboratory scale, with little ability to scale the system up to a viable large-scale manufacturing system. The process proposed needs to meet the desires of a very diverse consumer base whose need for these particles will vary. The process also needs to take into account the specific wants of the consumer (i.e. particle size, layer thicknesses, material selection) and the timely realization of the changes needed to improve the performance of the adaptive materials.

5.1 Implementing a Systematic Design Approach

In order to fully utilize the Pahl & Beitz approach, a gap analysis was performed to make use of the necessary tools and strategies needed to scale-up this manufacturing process and successfully sustain the process over a long period of time [64]. In order to do this, each shortcoming that was found in the original process is outlined. Then, a short proposal will be stated that outlines suggested solutions or strategies to account for the needs of the manufacturing process. The proposed approach is critically evaluated to ensure that it meets the needs of each of the established requirements and is feasible to apply to the manufacturing process. Finally, the results of applying the approach to the manufacturing process is displayed by drawing comparisons between the old manufacturing process and the new one in respect to cost, quality and efficiency.

5.1.1 Gap Analysis

The Pahl and Beitz approach was chosen due to the fact that it has been proven as an effective approach in the field of mechanical design for decades. The chosen approach works best because it provides one with the ability to internalize, customize, augment, and ultimately extend the baseline approach for one's own particular area of interest [64]. There are four phases to mechanical design process according to the Pahl & Beitz approach. The phases for the approach are:

- Planning and Task Clarification
- Conceptual Design
- Embodiment Design
- Detail Design

For this study, it is only required that the first two phases are covered since the goal is to build a concept for scaling up the manufacturing process for mass production.

Table 5.1 lists the steps to the planning and clarification phase of the approach. In addition to the steps are ideas for how the designer of would like to apply each step to the current manufacturing process. It is through this planning phase that the requirements necessary to build a concept are developed. The next phase depends on these requirements in order to ensure that all of the primary goals for the scale-up are met.

Table 5.1: Gap Analysis - planning & clarification of task

Planning & Task Clarification	
Phase Steps	*Application*
Analyze the Market & Company Situation	Consumer Needs: • Specialized Responsive Polymer Structures • Customizable Product (i.e. Size, Material) Manufacturer Needs: • Safe & Simple Process • Repeatable • Cost Effective
Find & Select Product Ideas	Various applications that utilize the abilities of the responsive particles and surfaces will be explored during research studies (i.e. selective capture, transport, controlled release & strain sensor)
Formulate a Product Proposal	Create a process that can be scaled up to meet the needs of a consumer base
Clarify the Task	Understanding how the product will be used, how much of the product needs to be delivered and how to market this product.
Elaborate a Requirements List	List of specific needs within the manufacturing process that is referred to upon designing the concept

By the conceptual design phase, the design approach requirements have been identified and there is a general idea of what needs to be accomplished. Most of the problems surrounding the process were solved in chapter 2 but need to be identified once again so that they can be evaluated on a large scale. It is the work in this phase that eventually becomes the concept which is evaluated at the end of this phase and in later phases. Table 5.2 lists the steps of the conceptual design phase along with how these steps can be utilized in the scale-up of the manufacturing process. Three of the five steps are explained in greater detail in the next section.

Table 5.2: Gap Analysis – developing the concept

Developing the Concept	
Phase Steps	*Application*
Identify Essential Problems	Problems to be analyzed: • Material Selection • Material Preparation • Layer Deposition • Curing • Cutting • Testing for Quality (i.e. Triggering)
Establish Function Structures	*Displayed in the Function Structure Diagram
Search for Working Principles/Structures	*Displayed in the Working Principle Chart
Combine & Firm up into Concept Variants	*Displayed in the Selection Chart
Evaluate Against Technical and Economic Criteria	Initial analysis is performed on large-scale manufacturing process for technical feasibility and cost. More rigorous analysis is performed during later design stages.

5.1.2 Modification Proposal

When dealing with complex systems that are new and innovative, it is necessary to devise ways to properly organize ideas and thoughts. In the affinity diagram shown in Figure 5.1, several ideas were presented on how to improve the manufacturing process. All of the ideas were brought together and organized into different areas where the process could be improved. From this list, certain areas were identified that would provide the largest improvement. Those areas were then placed as the headings of the affinity diagram and more specific solutions were identified and categorized. Tools such as affinity diagrams are helpful in organizing these ideas so that they can be addressed.

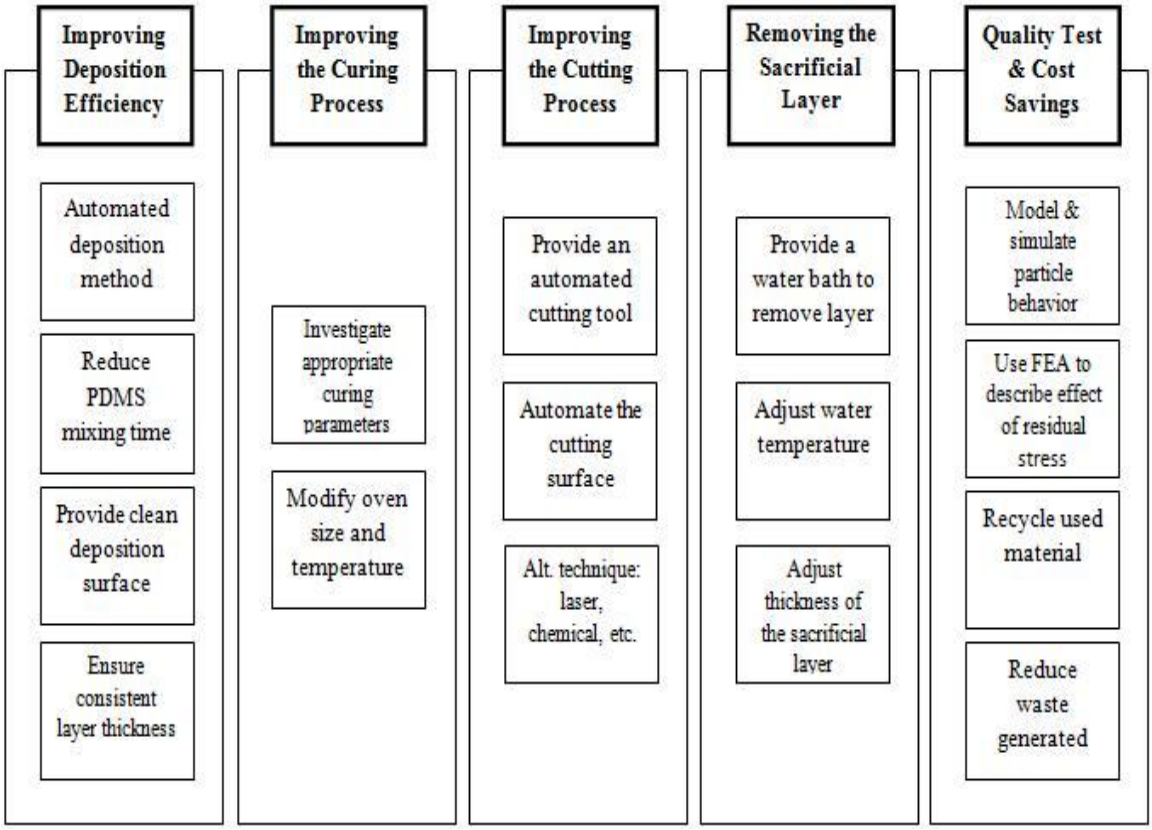

Figure 5.1: Affinity diagram

After looking at various methods for material deposition, curing, material cutting and quality assurance, a subset of principles was selected to test and improve. After accumulating data about the manufacturing process, a function structure diagram can be developed. The basic function structure diagram is based on the functional model displayed in Pahl and Beitz. In their approach, five generally valid functions and three types of flows are described in the chart at very high abstraction. Those three types were displayed as the overall flow of energy, material and signals within the system. More developed function structures can consist of as many as 30 functional descriptions which enhances the detail of the functional model of a design [65]. Using Figure 5.2, the aspects of the manufacturing process can be clarified and evaluated, which allows an improved concept solution to be developed [66].

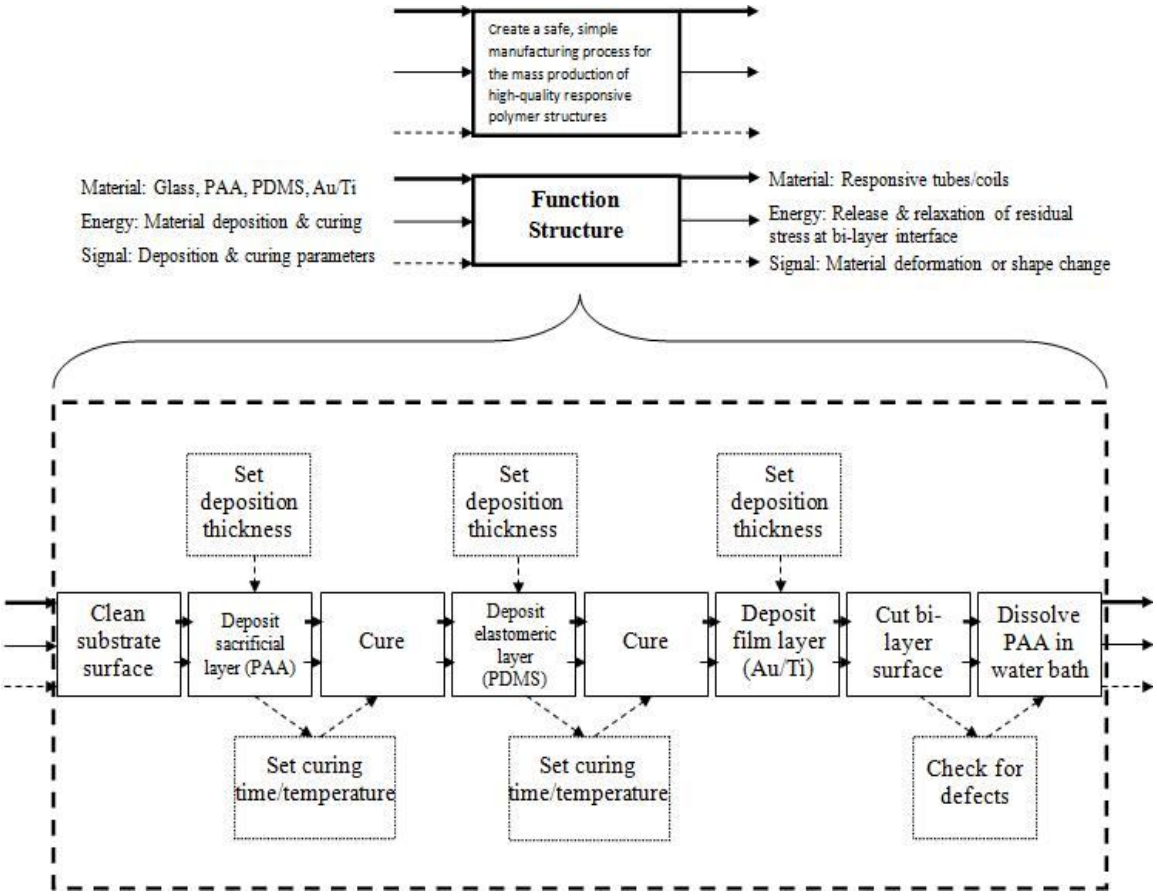

Figure 5.2: Function Structure Diagram

Several aspects of the manufacturing process could pose a problem. For instance, the separation of the particles into smaller, individual sections proved to be a problematic task in this study's manufacturing process. The original method involved the user using a razor blade to carefully cut the bi-layer into small sections. This method was not only dangerous and time consuming but also inefficient as far as being precise with the cutting dimensions. This was an area that was chosen to identify possible solutions for. Other problem areas include:

- PDMS preparation
- Layer deposition
- Curing time

- Dissolving the sacrificial layer
- Ensuring high quality particles

Using the function structure diagram, working principles and working structures can be seen and used to develop ideas for improving the existing process. This could include making the process faster, cleaner, minimize gaps between tasks or simply improve the quality of the final product. It is necessary to combine the working principles into a working structure in order to fulfill the overall function. This is accomplished by using Table 5.3 to list possible combinations of working principles that could result in an overall solution.

Table 5.3: Working principle chart

Subfunction/Solution	**1**	**2**	**3**	**4**
Material Deposition (A)	Manual Deposition	Push Nozzle (partially automated)	Automated Deposition Unit	
Curing (B)	Oven	Heated Surface (Hot-Plate)	Air Dry	
Cutting (C)	Manual Cutting	Automated Micro-Cutting Tool	Laser	Chemical
Dissolution (D)	Water Bath			
Defect Spotting (E)	Human Eye	Infrared Camera	Digital Smart	
Quality Testing (F)	Random Sampling	Behavior Simulation	Stress/Fatigue Testing (FEA)	

During this process, it was understood that all of the combinations must be compatible, technically feasible, and cost effective. One method for selecting working structures is through the use of a selection chart. The selection chart shown in Table 5.4 lists all of the function structures and rates each based on a set of criteria established by the user.

Table 5.4: Selection chart

Selection Chart					*Large-scale APP Manufacturing*		Part: 1 Page: 1	
Enter Solution Variant (Sv)	Solution Variants (Sv) evaluated by: <u>Criteria</u> (+) Yes (-) No (?) Lack of Information (!) Check Requirements List						Decision Mark Solution Variants(Sv) (+) Pursue Solution (-) Eliminate Solution (?) Collect Information (re-evaluate solution) (!) Check requirements list for changes	
	Compatibility assured	Fulfills demands of requirements list	Realizable in principle	Within permissible costs	Includes safety measures	Preferred by designer's company	Remarks (Indications, Reasons)	Decision
A1	+	-	-	+	-	-	*Too slow, unsafe*	-
A2	+	+	-	+	-		*Too slow*	-
A3	+	+	+	-	+		*Simple solution ; might be pricey*	+
B1	+	+	+	+	+		*Proven reliable solution*	+
B2	+	+	+	+	-		*Could be dangerous if not properly vacuumed*	-
B3	+	+	-	+	-		*Too slow*	-
C1	+	-	-	+	-	-	*Too slow, unsafe*	-
C2	+	+	+	+	+		*Hands-free ; faster*	+
C3	+	+	+	-	-		*Unsafe ; priciest option*	-
C4	+	+	-	+	-		*May not provide enough accuracy ; unsafe*	-
D1	+	+	+	+	+		*Cheapest option ; longer dissolution*	+
E1	+	-	-	+	+	-	*Not reliable*	-
E2	+	+	+	+	+		*More reliable ; price fairly reasonable*	+
E3	+	+	+	-	+		*Most reliable ; priciest*	-
F1	-	-	-	+	+	-	*Not a reliable method for quality assurance*	-
F2	+	+	+	+	+		*Needed for quality assurance*	+
F3	+	+	+	+	+		*Needed for quality assurance*	+

Even after the working principles are chosen, it is highly unlikely that the cost and production characteristics for the principle solution can be assessed from this analysis alone. This is usually covered in the later phases when the technical and economic evaluations are conducted, but for curiosity purposes, ideas on how each task in the manufacturing process can be scaled up are discussed in the next sections.

5.2 PDMS Preparation

The preparation of the elastomeric material creates a serious challenge in the design of the scaled-up manufacturing process. Preparing a polymer for a large-scale process poses many more challenges than creating the same material on a laboratory scale. This can be compared to preparing a meal for a large event or group as opposed to preparing that same meal for a small family in that the recipe needs to be modified in order to create a meal of equal quality. Tasks such as storing the materials, mixing and degassing need to be addressed as well as regular cleaning and maintenance of the equipment involved in this process.

The elastomer, PDMS (Sylgard 184^{TM}, Dow Corning Corp.) is provided in a silicone elastomer kit consisting of a viscous elastomeric base (pre-polymer) and a thin cross-linking agent. The manufacturer of the material recommends that the elastomeric base and cross-linking agent is mixed at a 10:1 ratio, respectively. Upon mixing of the two materials, polymerization begins and the material begins to cure. It is for this reason that proper storage of the two materials is a critical factor in the preparation of this material on a large-scale. There are at least two approaches that someone designing this step in the process can take. In both approaches, it is important that the elastomeric base and cross-linking solutions are stored separately and in an environment that will prevent dust, moisture or other impurities from contaminating the solutions. In the first approach, the elastomeric base can be stored in a storage bin and stirred continuously by an

industrial-sized stirrer. The cross-linking agent is, then, measured and added manually by an operator through a door that can be opened at the top of the storage bin. After a certain amount of time, the cross-linking agent is sufficiently dispersed amongst the elastomeric base, and the solution is pumped into another compartment for degassing and deposition.

The second approach is slightly more automated in that it does not require an operator to actively participate in the process. This approach consists of a four-compartment system where each material is stored in separate environmentally-controlled compartments. Each compartment is connected to a pump that periodically adds a pre-determined amount of material from each compartment to a third compartment where the two solutions are combined by a continuously turning mixer. After adequate mixing, the material is pumped to a final compartment that is under high vacuum to remove any air or gas that may have entered the solution during mixing. The degassed material is pumped into a set of automated deposition nozzles to begin the next step of the process. A schematic of this approach is shown in Figure 5.3. Though an operator would not be needed for this approach, operators would be needed to clean the compartments, periodically, to prevent cross-contamination or blockage in the third and fourth compartments due to cured material that was not deposited in the next step. Also, regular maintenance to the pumping system would be required to minimize stops in the process.

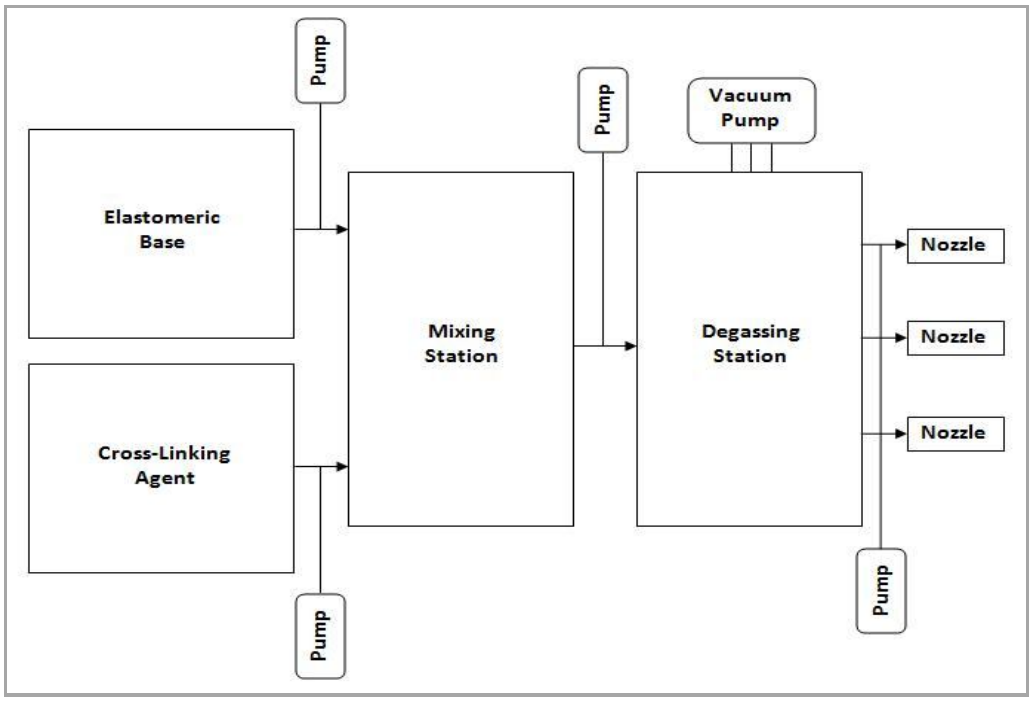

Figure 5.3: Automated PDMS preparation approach

5.3 Layer Deposition

Based on the analysis provided while utilizing the planning and design tools in the systematic approach, material deposition would require, at least, some automation in order to scale-up this task within the manufacturing process. Logically, a completely automated process would be considered the most effective in achieving this goal, but the cost of implementing such ideas should be monitored to ensure that they add value to the final product. A typical layout for this process would work similar to an automotive assembly line. There would be operators for each task to ensure that the machinery is running properly. Also, a creative set-up needs to be established to minimize stops in the line. The bi-layer structure would be built on a conveyor line where automated depositors would apply a pre-determined amount of material for the sacrificial layer. The conveyor line would consist of rotating surfaces that would simultaneously spin cast the layers as the material was deposited as shown in Figure 5.4.

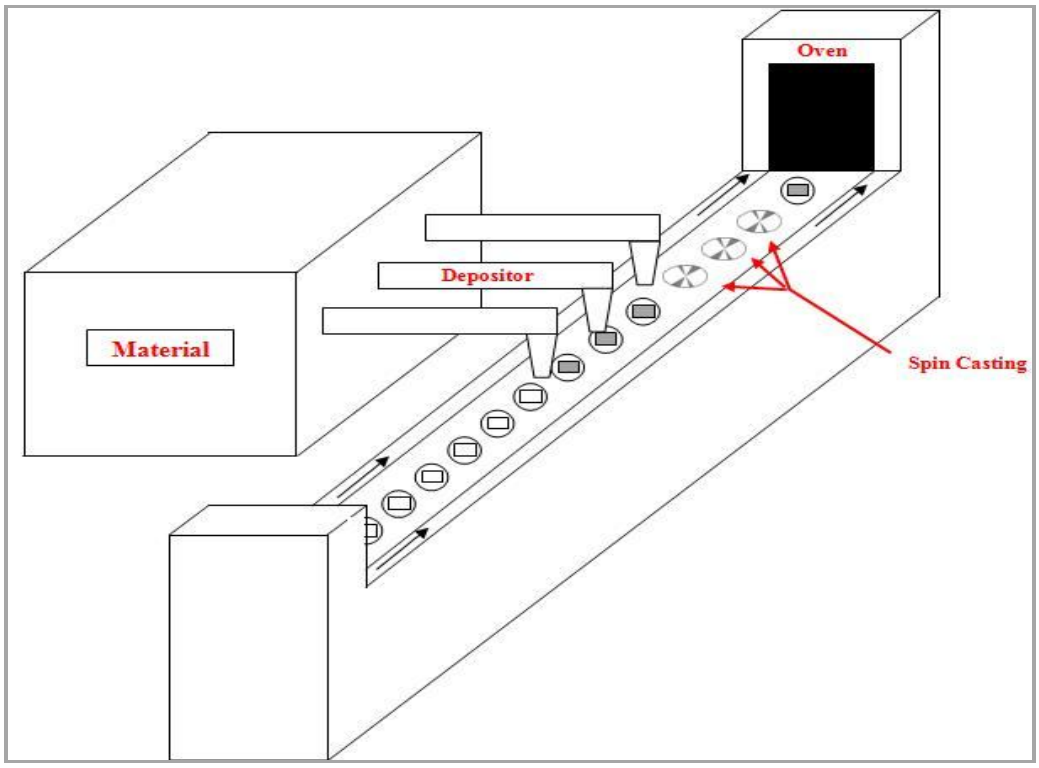

Figure 5.4: Large-scale manufacturing conveyor concept

The first material to be deposited is the sacrificial layer, Polyacrylic Acid (PAA 20% wt aqueous solution, Sigma-Aldrich). Since the PAA does not require any pre-mixing or degassing, an elaborate pre-preparation step is not needed. The PAA is simply stored and deposited on each glass surface as they move along the conveyor line. Each sample is placed on a disk-shaped surface that can be rotated to high speeds by small motors under the surface. Depending on the viscosity of the material that was deposited and the preferred thickness, the speed at which the motor spins the surface can be preset. Since the material thickness is time and speed dependent, the length from the spin-casting cycle to the entrance of the curing oven on the conveyor line can be lengthened or shortened to account for the time needed to reach the desired thickness. After the sacrificial layer is spin-cast on the deposition surface, the sample enters its curing phase which will be discussed in more detail shortly. After the sacrificial layer is completely cured, the conveyor carries the samples to the next set of depositors which add the

appropriate amount of elastomeric material on top of the cured PAA and glass surface. A second spin-casting cycle immediately follows the deposition of the elastomeric material and the samples are sent through a second industrial sized oven in order to cure the elastomer. After the elastomeric material is completely cured, an operator removes batches of the samples and brings them to a separate station for electron beam evaporation if the top film layer is a metal. For organic films layers, a separate manufacturing line can be created to add an additional deposition, spin-casting and curing station similar to the one used for the other layers.

5.4 Curing

As discussed earlier, curing plays an important role in the responsiveness of the particles. It is important that this task within this automated process can be effectively scaled up to consistently produce cured bi-layer structures that are of high quality. For this step in the process, the structures will enter a series of industrial-sized ovens that are set to the appropriate temperature for curing each deposited layer. The length and size of each oven will be dependent on the speed at which the conveyor moves relative to the amount of time needed for the material to completely cure at a specified temperature. After leaving the oven, the conveyor line takes the structure to a next set of depositors that would apply another layer. Once again the automated rotating surfaces would be activated and the next layer (i.e. the elastomeric material) would be evenly dispersed. After each curing cycle, an operator can perform an inspection to verify that the layers are at the appropriate thickness. Since the layers are too thin to be inspected by eye, operators would have to randomly inspect certain samples via profilometer.

5.5 Cutting

After film deposition, the newly-formed bi-layer structures are cut using an automated micro-drilling apparatus like the one shown in Figure 5.5. The cutting surface

can be detected by a laser that is erected above the conveyor surface and used to accurately predict the point of contact and depth of cutting for each sample. The cutting tools used for this task are 2-flute micro end mills (Performance Micro Tool) with cutting diameters that range from 30 um to 150 um. The cutting tools are positioned inside of a drilling apparatus that is capable of rotating the tool up to 60,000 rpm. Since these micro tools have a limited tool life, an operator would have to monitor the tool and cutting surface and perform regularly scheduled tool changes to ensure that the cutting tool is performing at its optimum capability. Upon reaching the cutting station, the workpiece has to come to a complete stop on the conveyor line. Next, the set of bars hold the workpiece stationary while the laser locates the point where the cutting process will begin. Finally, the cutting head, which would have axes of motion in the x, y and z direction, makes contact with the cutting surface and begins to cut a predetermined pattern that is programmed by the computer which controls the automated unit. The speed at which the cutting head moves along the surface of the sample will determine how long this process will take.

Figure 5.5: Automated micro-drilling tool (Courtesy of Dr. Shreyes Melkote)

5.6 Removing the Sacrificial Layer

The final step involves dissolving the sacrificial layer by dropping the cut bi-layer into a water bath. This step is normally performed in a small beaker with one or two small (25.4 mm x 76.2 mm or 50.8 mm x 76.2 mm) samples, but for this large scale process, an industrial sized water bath would be needed to remove the sacrificial layer of several samples at once. Since the rate of dissolution of PAA is solely dependent on the thickness of the layer deposited, the thickness of the layer will be kept at a minimum in the prior steps. Once the PAA is dissolved away, newly formed three-dimensional micro- and nano- responsive structures are formed. Not only do these structures have the tendency to float on water, but these particles also follow a flow field. These two characteristics can be taken advantage of in this final task through the use of a small pump that can be set up near the top of the water bath. The vacuum would create a flow path that pulls newly formed particles out of the water bath where they were formed and transports them into a separate unit for the final inspection or any analysis that needs to be performed to ensure that the particles are to the satisfaction of the consumer.

CHAPTER 6

RESPONSIVE SURFACES

In addition to the manufacturing of responsive particles using strain engineering, the concept of strain recovery of the elastomeric material was utilized to create a responsive surface using PDMS. Previous studies have shown how strain can be used in altering certain characteristics in responsive surfaces [9, 13, 14, 52, 55]. Specifically, work in producing elastic circuits that are able to perform under high strains have opened the door for the development of surfaces that have the ability to sense changes in their environment and respond accordingly [10]. Therefore, an additional study was performed and included in this thesis to investigate the development of nanocomposite-reinforced polymer strain sensors. In this study, the goal was to develop a strain sensor in a simple and cost effective way that can be applied to a number of small mechanisms without hindering the design or applying large loads.

6.1 Strain Sensors

Many of the strain sensors produced today are made from stiffer, more expensive materials than the materials proposed for this study. It is the bulk and expense of these materials that limit the potential application of many of these sensors [67, 68]. Thin film sensors are relatively small and can be applied to a number of small mechanisms without hindering the design or applying large loads. These sensors can be applied to numerous applications which include actuators, switches and microelectronic devices that detect mechanical and thermal strain. This makes small-scale strain sensors especially favorable for use in the aerospace industry where efficient strain monitoring units that do not hinder the operation of large mechanisms, such as aircraft components, are needed.

These sensors were created by casting vapor-grown carbon fiber (VGCF) reinforced PDMS. When sufficient VGCFs are added to PDMS, the resulting film is electrically conductive. There is, however, a certain threshold value at which enhanced electrical properties can be observed. When concentration values exceed the threshold concentration, PDMS/VGCF films should act as a type of circuit, which allows a current to pass through it easily. This is achieved due to the fact that the tightly packed conductive fibers form networks throughout the polymer matrix. This network becomes stronger when additional fibers are added. Upon applying strain, these fibers are spread apart and the conductive networks are broken, but the network can be reestablished once the strain is removed [69]. The idea is that a sensor can be created that can measure the strain the material surface is under by monitoring the electrical resistance.

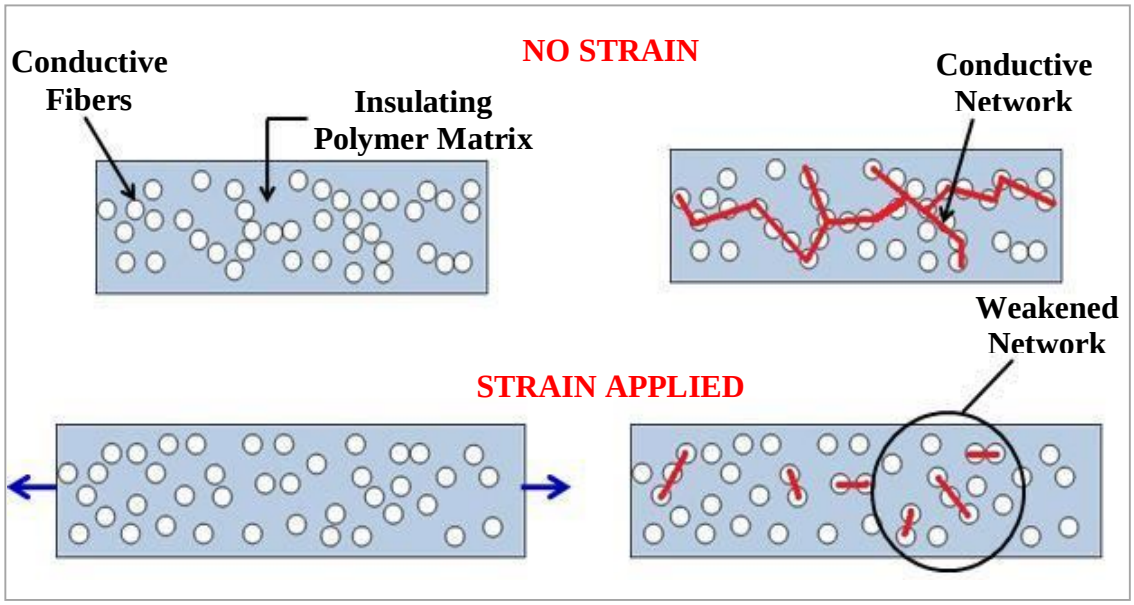

Figure 6.1: PDMS-VGCF strain sensor mechanism

Previous studies have observed a relationship between the electrical conductivity of a composite material and mechanical strain [69]. Determination of the relationship between the electrical resistance of the film and the applied strain can lead to a calibration curve for the strain sensor. In addition, if these surfaces are to be considered

as strain sensor candidates for an application, they need to display qualities of durability and repeatability.

6.2 Strain Sensor Fabrication

VGCFs offer an inexpensive alternative to carbon nanotubes (CNTs). Each have been used as filler material and display comparable enhancements of electrical, mechanical, and thermal properties. In regards to electrical properties, VGCFs display electrical conductivity enhancements of up to 12 orders of magnitude higher than that of single-walled carbon nanotubes (SWCNT) [70]. VGCFs have also proven to be very useful in electronic devices and in enhancing the mechanical properties of composite materials [71, 72]. Most importantly, VGCFs have the ability to transform insulating polymers into electrically conductive polymers without significantly altering any of the polymer's properties.

Just like in the development of the responsive particles, the first step in developing a strain sensor was to create a basic manufacturing process. The PDMS/VGCF nanocomposites were created using a simple film fabrication process involving PDMS (Sylgard 184^{TM}, Dow Corning Corp.) silicone elastomer kit and various concentrations of VGCFs (PR-19 AG grade, fiber diameter 100 to 200 nm and 30 to 100 um in length, Pyrograf Products Inc.). The base material was fabricated by mixing the appropriate quantities of PDMS elastomer base and VGCFs. This mixture was stirred by hand using a glass pipette for 20 minutes or until the solution is visibly homogeneous to ensure a thorough dispersion of the VGCFs [73]. Next, the PDMS curing agent was added to the mixture at an elastomer base to curing agent ratio of 10:1 and stirred for an additional 20 minutes. Once the PDMS/VGCF composite materials are properly mixed,

thin films are created by pouring the solution into pre-made molds as shown by Figure 6.2 below. Seven specimens with varying concentration of VGCFs (0, 1.5, 2.0, 2.5, 3.0, 3.5, 4.0) were prepared for this study.

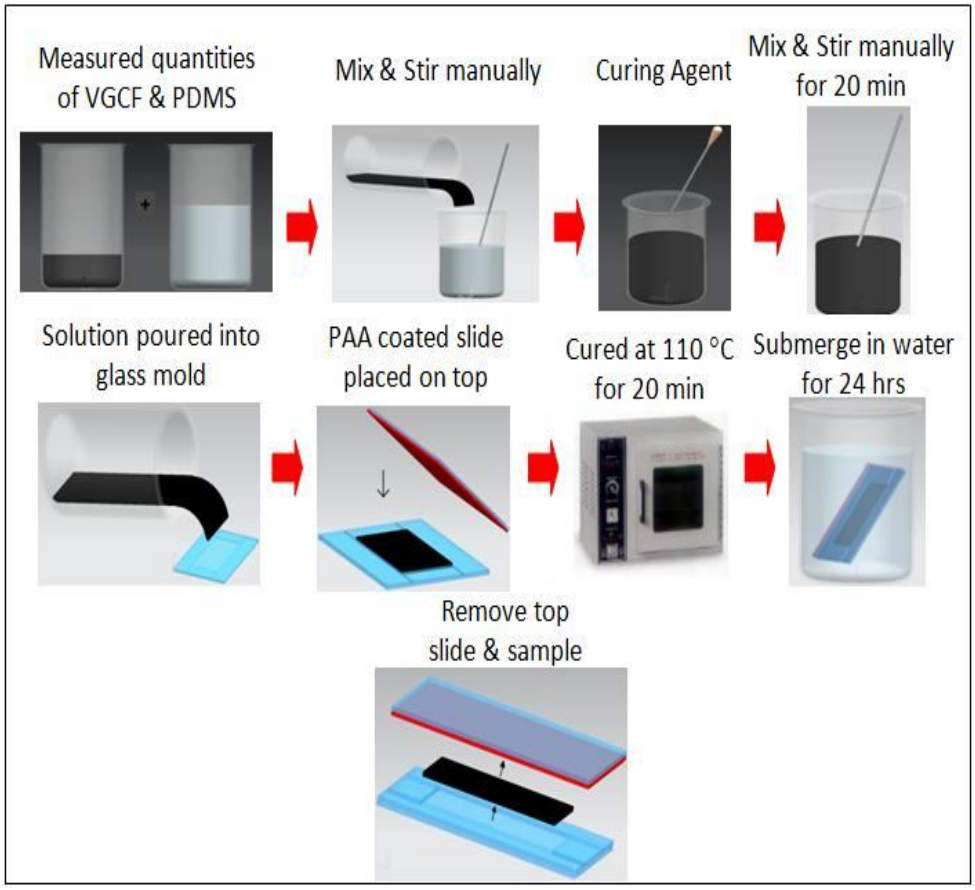

Figure 6.2: Manufacturing process for PDMS/VGCF thin films

The molds were created using standard glass microscope slides to allow the composite to take the form of a cavity that was 50.8 mm (2") long, 25.4 mm (1") wide, and approximately 1.5 mm thick. The solution was allowed to degas under a fume hood for about 40 minutes. While the solution was degassing, polyacrylic acid (PAA) was spin cast (WS-400-6NPP Laurell Spin Coater) onto a separate glass slide at 1200 rpm for 2 minutes. Next, the PAA coated slide was placed directly on top of the glass mold cavity to flatten both sides of the film and the mold was cured at 110°C for 20 minutes. After

the sample had been cured, it was placed in a container of water for 24 hours. During this time, the water breaks down and dissolves the PAA. Submerging the sample in water drastically increases the ease of detaching the top slide from the mold because the PAA is soluble in water. Finally, the sample was removed from the water, top slide detached and the thin film was carefully cut from inside the mold cavity to dry.

6.3 Strain Sensor Characterization

Mechanical analysis of the composite material was conducted to determine the stress-strain relationship, modulus of elasticity and enhanced mechanical capabilities of the material at different weight percentages of VGCF. This was performed using a Q800 DMA (TA Instruments). Tensile tests were performed and the DMA was programmed to operate in strain rate mode. All specimens were cut to the same dimensions (20 mm x 6 mm x 1.5 mm) and subjected to a tensile load at an isothermal temperature of 30°C. The test applied strain to each film at a rate of 1% per minute until a maximum strain of 25% was reached. While applying strain, the instrument recorded stress, deformation, and static force. The Young's modulus of the PDMS-VGCF films for various loadings of VGCF was determined based on the slope of the stress-strain curve and is shown in Table 6.1

Table 6.1: The effect of VGCF concentration on composite modulus

VGCF Weight Pct.	Average Young's Modulus (MPa)	Standard Deviation
0	2.61	0.35
1.5	3.14	0.20
2.0	3.48	0.19
2.5	3.86	0.28
3.0	3.82	0.25
3.5	4.02	0.10
4.0	4.55	0.18

The Young's modulus increased with VGCF concentration and none of the films failed after being subjected to a maximum strain of 25%. 25% strain equates to a maximum deformation of approximately 1.7 mm for each of the samples. This is important because it shows that these films are able to withstand high pressures and deformations, while simultaneously having enough elasticity to deform and return back to their original shapes upon release of the mechanical load.

Although tensile strength increased with the addition of VGCF, elasticity and flexibility decreased. These are key components in producing effective strain sensors. If the films are not able to bend or tolerate tensile and compressive stresses, severe limitations in applications can arise. These films must be able to adhere to a wide variety of surface designs as well as respond to changes that might occur on a surface such as cracks or thermal expansion. In order to be successful in sensor production, a medium must be found that produces a material that can show efficient elasticity, excellent conductivity and is not hindered by the various forms of stress that the material might be subjected to in application.

The electrical resistance was measured using a SI 1287 Electrochemical Interface and 1255B Frequency Response Analyzer (Solartron). Two tests were performed with these units. The first was performed with no strain applied to each sample to determine the relationship between VGCF percentage and resistance as well as the percolation threshold. The second test was performed at different percentages of strain to produce a plot that relates the electrical resistance to the mechanical strain. Before taking measurements, each end of the rectangular composite specimen was fixed between two

insulating pads to ensure that the electrical resistance measurements would not be affected by the aluminum holding apparatus shown in Figure 6.3 below.

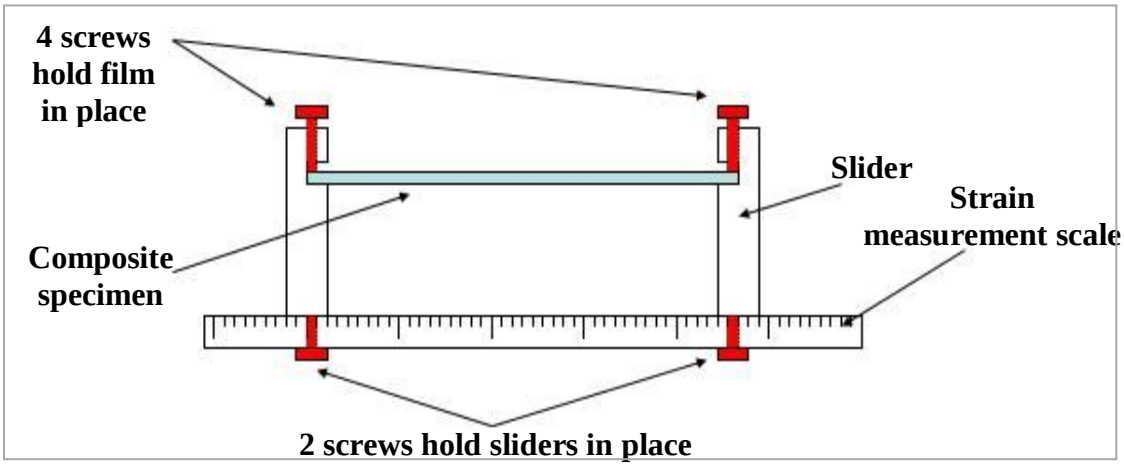

Figure 6.3: Strain sensor holding apparatus

The volumetric electrical resistance of each sample was measured using a standard four-electrode (FE) method [74, 75]. The SI 1287 Electrochemical Interface and 1255B Frequency Response Analyzer (Solartron) testing set up consists of two alligator-clip electrodes that clamp to the sample. The electrical current (I) was set to 30 mA and maintained in all measurements. Also, the apparatus was set to cycle from an initial frequency of 10^5 Hz and a final frequency of 10^{-1} Hz and move in intervals of 5 points per decade. Before each run, the distance between the electrodes along with the width and thickness of the sample were recorded. Measurements were, initially, taken with no strain to obtain the resistance of the specimens that were prepared for testing. The apparatus measured the resistance of the composite material which is shown in Table 6.2.

Table 6.2: The effect of VGCF concentration on composite electrical resistance

VGCF Weight Pct.	Resistance per Unit Length (Ω/mm)	Standard Deviation
0	1.15×10^{13}	1.94×10^{12}
1.5	1.40×10^{8}	1.10×10^{7}
2.0	2.25×10^{4}	7.04×10^{3}
2.5	4.81×10^{2}	3.92×10^{1}
3.0	4.25×10^{2}	3.91×10^{1}
3.5	2.36	2.39×10^{-1}
4.0	2.24	6.90×10^{-2}

The tests show that the conductance is enhanced at small percentages of VGCFs. Figure 6.4 shows the effect VGCF concentration has on both the mechanical and electrical properties of the PDMS-VGCF films. From the data, it can be seen that the modulus steadily increases as the percentage of VGCFs in the material increases. Meanwhile, a similar trend was seen in the resistance (all errors are within 10%). More importantly, there was a significant drop in resistance between 1.5% and 2% VGCF concentration. The significant drop in resistance suggests that the percolation threshold is between 1.5 and 2 wt. % of VGCF. The percolation threshold is the point at which the fibers in the polymer matrix form a network allowing the flow of a current through the material.

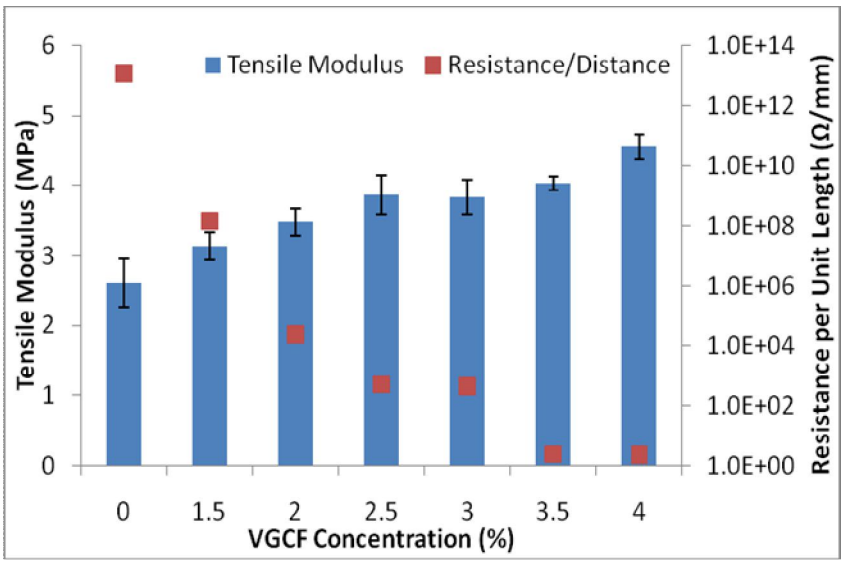

Figure 6.4: Effect of VGCF concentration on tensile modulus and resistance of a composite

Ideally, as strain is applied, the conductive network should weaken and the conductance should drop [76, 77]. Upon removal of the strain, the conductance should return back to the initial state. In reality, this is only partially true. As Figure 6.5 displays, the resistance of the surface never completely recovers even after the load is removed.

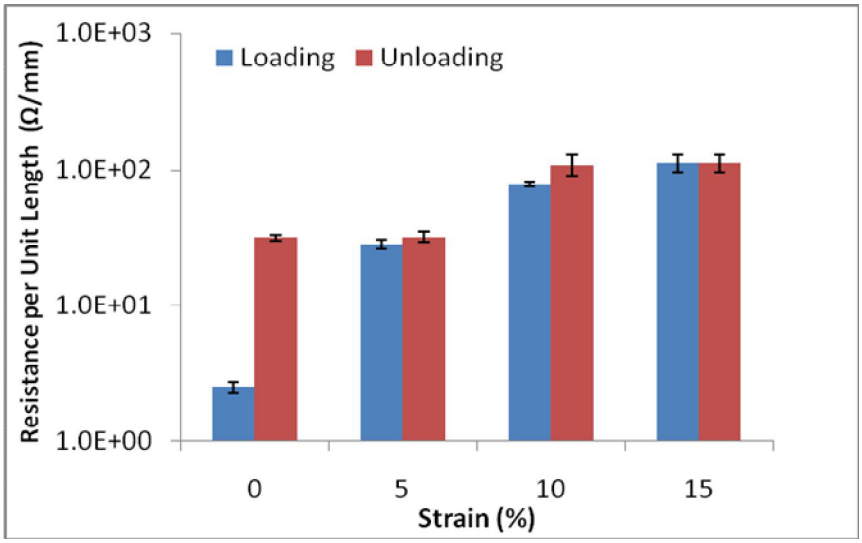

Figure 6.5: Effect of strain on the electrical resistance of a composite material

It is apparent that there is a rise in resistance during loading, but as the strain is slowly removed, the resistance is never able to return back to its initial state. This trend was seen for all concentrations of VGCF used in this study. These results can be attributed to a number of factors including the maximum amount of stress the conductive fibers are able to handle and the fact that the polymer matrix might be too flexible in that it does not allow the fibers to realign. Also, it is suspected that energy is lost during the loading and unloading process. Since the sensors were stretched by as much as 15%, many of the fibers may have been deformed to the point that they are not able to reconnect in a network. In addition, the base material, PDMS, might require more rigidity to reduce deformation of the conductive network. Many of these reasons contribute to energy from the conductive network being lost or dissipated through the insulating polymer matrix during loading cycles.

To verify this hypothesis, additional tests were performed with VGCF composite specimens made with different amounts of elastomer base to cross-linking agent ratios. More test specimens were fabricated using the recommended 10:1 ratio and additional test specimens were fabricated using 10:1.5 and 10:2 mixing ratios to improve the strength of the polymer matrix. For this trial, only VGCF concentrations of 3% and 4% by weight concentration were studied since they were well above the percolation threshold. Also, strain testing was performed up to 5% as opposed to 15% strain. Figure 6.6 shows how the Young's modulus of each specimen changes when the mixing ratio and VGCF concentration is increased. It is shown in Figure 6.6 that the test specimens at higher ratios have a higher modulus as expected.

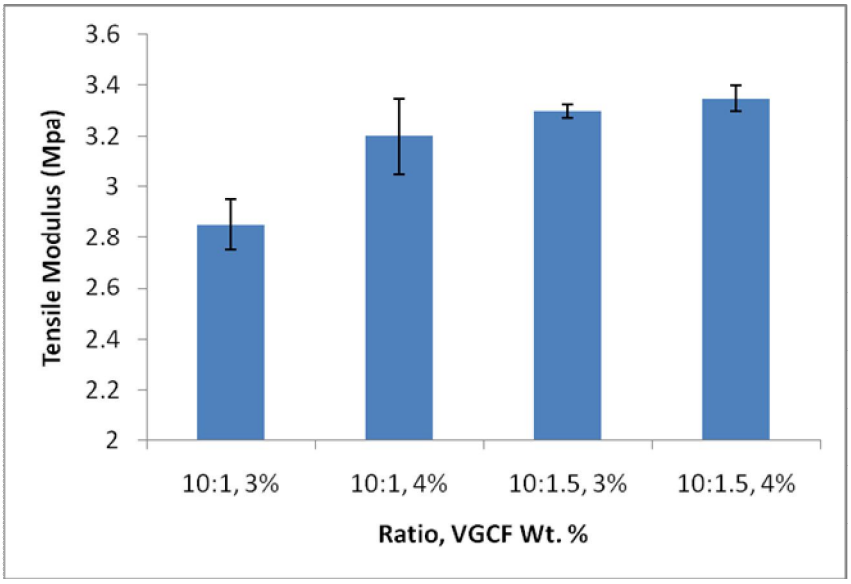

Figure 6.6: Effect of VGCF concentration and cross-linking agent ratio on tensile modulus

To verify the second part of the hypothesis, each specimen is once again placed under stretching and relaxation cycles to confirm the consistency of the previous data and observe whether or not the increased amount of curing agent reduces the amount of energy dissipated. Figure 6.7 shows the electrical resistance data (all error values are within 10%) for the specimens at the higher elastomer base to cross-linking agent ratios. Comparing this data to the previous data in Figure 6.5 shows that the increase in ratio does have an effect on how the conductive fiber network responds under repeated loading and unloading.

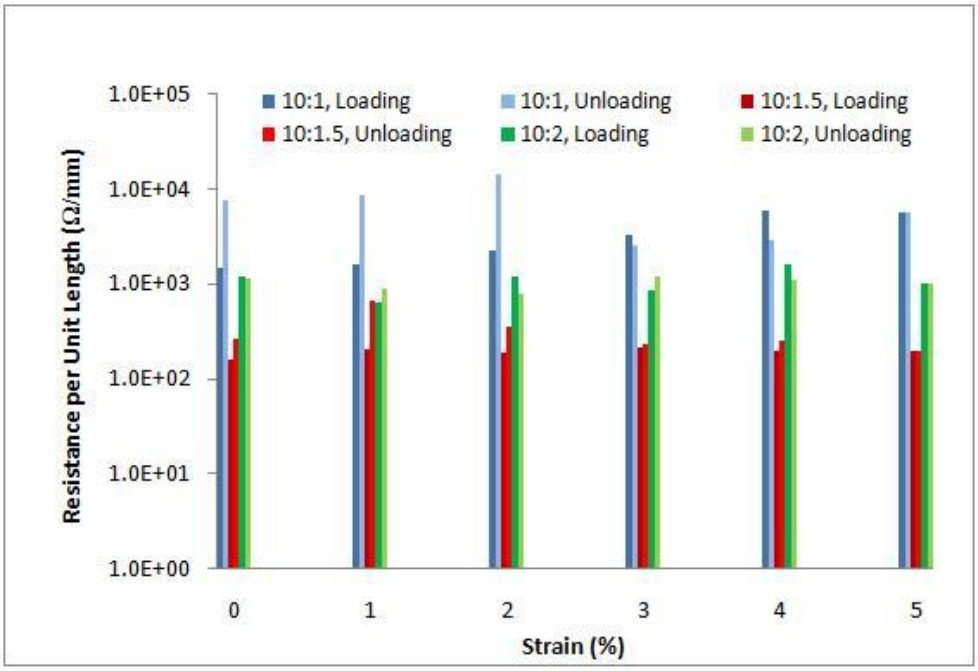

Figure 6.7: Effect of cross-linking agent ratio on electrical resistance for 3% VGCF

This study shows that the concept of strain recovery of an elastomeric material such as PDMS could be utilized to create a strain sensor. This study provided the first steps for using such materials for this application. These strain sensors were created by mixing various concentrations of VGCFs in a PDMS base. The mechanical and electrical properties were examined and the percolation threshold of these films was found. Strain was applied to these films to determine the relationship between the electrical resistance of the film and the applied strain so that a calibration curve for the strain sensor could be established. At high strains and a low elastomeric base to cross-linking agent ratio, it was found that the conductive fibers were unable to reestablish a network upon unloading the strain. Therefore, higher mixing ratios were used to improve the recovery of the conductive fiber network. At the PDMS mixing ratio of 10:1.5, there is still a lack of recovery in the conductance of the PDMS-VGCF films, but at the mixing ratio of 10:2, the resistance of the PDMS-VGCF films does not show much change during loading.

This suggests that there may be an elastomeric base to cross-linking agent ration between 10:1.5 and 10:2 that might provide a better base for the conductive filler material. Another option would be to use a bulkier conductive filler material that would make the elastic recovery process simpler.

CHAPTER 7

CONCLUSIONS

In this study, the principles of strain engineering were tested and used to develop a manufacturing process for the creation of responsive particles. This involved the proper selection of materials in manufacturing a thin bi-layer structure and the development of a simple manufacturing process that addressed the material preparation, deposition, curing, cutting and removal of the sacrificial layer. The characterization of the responsive particles as well as the demonstration of the responsive properties of the particles was also discussed. Ultimately, these particles were used in a basic application that utilized their ability to capture, transport and release another substance on command and a large-scale method for mass producing these particles was developed. The findings of this research have helped to further the study of strain engineering and how it can be used as a tool in triggering a response in structures composed of various materials.

7.1 Findings

This work addressed many of the problems associated with building a thin multi-layered structure. In covering the fabrication and mechanical characteristics of the structures, this analysis provided many interesting findings that provided the basis for understanding the mechanics behind this strain engineering method. These results include:

- Providing an understanding of how the processing conditions of the manufacturing process effect the characteristics and quality of the responsive particles

- Characterization of the responsive bi-layer structures and the resulting particles
- Demonstration of the particles ability to reversibly respond to a stimulus
- A systematic approach for the large-scale production of responsive particles
- The development of strain sensors utilizing strain recovery of an elastomeric material

During the development of the manufacturing process for the bi-layer structure, PDMS was used as one of the layers due to its responsive properties which made it suitable for creating these structures. In preparing the PDMS for deposition, it was found that the thickness, modulus and uniform mismatch strain of PDMS could be controlled through the processing parameters of the manufacturing process. Thinner layers of PDMS could be fabricated using three techniques:

- Increasing the spin rate of the spin casting process
- Increasing the time of the spin casting process
- Diluting the PDMS solution with hexane

Adjusting the spin rate and spin time of the spin casting process was and still is a common method for fabricating thin layers, but diluting the PDMS solution provided an additional way to reduce the layer thickness by reducing the viscosity of PDMS.

In addition to controlling the deposited thickness of PDMS, the modulus of the elastomer could be controlled by i) diluting the PDMS solution and ii) changing the curing temperature. Each method provided a means of controlling the modulus of the PDMS layer which, in effect, allowed for a means of controlling the size of the particles that were produced from the bi-layer structure.

Finally, controlling the uniform mismatch strain at the interface of the elastomeric layer and the top film layer was discussed. This was done by i) degasification of the PDMS solution and ii) observing PDMS shrinkage as a result of curing temperature. It was found that the amount of residual stress created by the mismatch strain was opposed by the increasing modulus of the PDMS layer. Therefore, the search for an optimum curing temperature was performed.

Four material layers were studied as suitable top film layer in the bi-layer structure to see which material systems work best in creating responsive particles. These materials included:

- Parylene – C
- SiC
- Oxidized PDMS
- Au/Ti

The study showed that organic and metallic films could be used to build responsive bi-layer structures as long as the material formed a close bond to the elastomer and had at least one property that differed enough from PDMS to be exploited by a stimulus.

The challenges that cutting the bi-layer structure posed allowed for the investigation of automated cutting processes. Both laser cutting and micro-machining were examined and found to be reasonable approaches for completing this task.

Triggering the response of the bi-layer structures created in this study was discussed along with the various types of triggering methods. The two triggers evaluated in this study were temperature and solvent. Each provided motivation to develop new responsive structures that could utilize different stimuli.

During the characterization of the responsive particles, it was found that many of the processing parameters established during the manufacturing of the bi-layer effectively controlled the final state of the particles. Each of the following factors were found to effect the final particle size:

- Modulus of PDMS
- Layer thickness of PDMS
- Top thin film deposition rate

As discussed prior, it was found that the modulus of PDMS could be increased simply by increasing its curing temperature. It was revealed that increasing the modulus i) increased the stiffness of the PDMS layer resulting in an increase in particle size and ii) reduced the effect of residual stress in the bi-layer. The discovery of these factors led to the idea of an optimum curing temperature in which both attributes could be controlled to minimize particle size. It should also be noted that techniques such as diluting the PDMS solution prior to curing reduces the modulus. In addition to reducing the modulus, diluted PDMS forms thinner layers which were found to reduce the size of the particles created from the process.

It was also shown that PDMS was not the only layer that affected the particles size. Increasing the rate of deposition of the top film layer resulted in the material being deposited under a greater amount of stress resulting in smaller particles. As the deposition rate of Au/Ti was increased from 1 A/s to 3 A/s, the size of the resulting particles were reduced.

PDMS-SiC and PDMS-Au/Ti particles were fabricated with identical processing parameters and compared. In analyzing the different material systems, it was determined

that the characteristics of the bi-layer structure changes depending on the material system being used due to the difference in material properties.

Rheology was used to demonstrate the responsive properties of the particles produced from the bi-layer structures. The opening and closing of the particles was demonstrated through changes in the viscosity of the fluid medium in which the particles were dispersed. A rise and fall in viscosity was evident as the particles opened and closed during two heating and cooling cycles. This proved that the response of the particles was reversible.

Upon creating the particles from the bi-layer structure, their ability to be used as a delivery vehicle was tested in a novel application involving the selective capturing, transport and release of a polymer. Such an application provided insight into the potential of these responsive particles.

With a greater understanding of the importance of each step in the fabrication of the bi-layer structure as well as the development of novel techniques, an example of how a systematic design approach could be used to scale-up the current manufacturing process was discussed.

In addition to the analysis performed on responsive particles, an additional study was performed for the development of responsive surfaces. It was also shown that PDMS could be infused with conductive fibers and used to create a composite material that responds to changes in strain. These responsive surfaces provided promising candidates for small-scale strain sensors.

7.2 Limitations & New Challenges

There were many issues surrounding the manufacturing and characterization of the responsive particles. Many of these issues were addressed during this work. Unfortunately, this study did leave some questions unanswered in the analysis of these structures. The limitations of this study include:

- Extensive evaluation of only 1 stimulus type was provided
- Only 4 material systems were covered
- Methods for demonstrating particle responsiveness were limited

The study only covered the manufacturing and characterization of thermo-responsive particles. As expressed in the literature, there are many responsive materials that respond to different stimulus types, yet this study decided to focus primarily on temperature. In addition, this study only covered four different material systems that could be used to create the responsive particles. More options will need to be explored in future studies to show the versatility of this process. Additionally, more methods for demonstrating the responsiveness of these particles need to be developed. This study only covered two demonstrations (i.e. viscosity and light absorption), but there are other properties that could be examined that are affected by the particles' change in geometry.

With that being said, there is still much work to be done on the subject of strain engineering and the development of responsive particles and surfaces. By understanding how these materials work, new ways of controlling the response of structures made from responsive materials can be discovered. The challenges that wait in the future with this study are perhaps explained best by the statement below:

Though stimuli responsive polymers are attractive for their potentials, they have to overcome several barriers: rapid response, mechanical strength, reproducibility, biocompatibility, biodegradability, non-toxicity and so on [48].

This challenge provides the motivation to continue thinking of ways to topple these barriers and open the doors to more common applications to benefit society. Hopefully, the work produced for this thesis provided significant contribution towards this effort.

REFERENCES

1. Martyniuk, M., et al., *Stress in low-temperature plasma enhanced chemical vapour deposited silicon nitride thin films.* Smart Materials & Structures, 2006. **15**(1): p. S29-S38.

2. Rim, K., et al., *Strained SiCMOS (SS CMOS) technology: opportunities and challenges.* Solid-State Electronics, 2003. **47**(7): p. 1133-1139.

3. Ghyselen, B., *Strain engineering in SOI-type materials for future technologies.* Materials Science and Engineering B-Solid State Materials for Advanced Technology, 2005. **124**: p. 16-23.

4. Guan, J.J., et al., *Self-folding of three-dimensional hydrogel microstructures.* Journal of Physical Chemistry B, 2005. **109**(49): p. 23134-23137.

5. Guan, J.J., et al., *Fabrication of particulate reservoir-containing, capsulelike, and self-folding polymer microstructures for drug delivery.* Small, 2007. **3**(3): p. 412-418.

6. Golod, S.V., et al., *Fabrication of conducting GeSi/Si micro- and nanotubes and helical microcoils.* Semiconductor Science and Technology, 2001. **16**(3): p. 181-185.

7. Stoney, G.G., *The tension of metallic films deposited by electrolysis.* Proceedings of the Royal Society of London Series a-Containing Papers of a Mathematical and Physical Character, 1909. **82**(553): p. 172-175.

8. Lacour, S.P., et al., *Stretchable gold conductors on elastomeric substrates.* Applied Physics Letters, 2003. **82**(15): p. 2404-2406.

9. Jones, J., et al. *Stretchable wavy metal interconnects*. 2004: A V S Amer Inst Physics.

10. Lacour, S.P., et al., *Stretchable interconnects for elastic electronic surfaces.* Proceedings of the Ieee, 2005. **93**(8): p. 1459-1467.

11. Li, T. and Z. Suo, *Ductility of thin metal films on polymer substrates modulated by interfacial adhesion.* International Journal of Solids and Structures, 2007. **44**(6): p. 1696-1705.

12. Kim, D.H. and J.A. Rogers, *Stretchable Electronics: Materials Strategies and Devices.* Advanced Materials, 2008. **20**(24): p. 4887-4892.

13. Lacour, S.P., et al., *Mechanisms of reversible stretchability of thin metal films on elastomeric substrates.* Applied Physics Letters, 2006. **88**(20): p. -.

14. Kim, D.H., et al., *Stretchable and foldable silicon integrated circuits.* Science, 2008. **320**(5875): p. 507-511.

15. Ahn, B.Y., et al., *Omnidirectional Printing of Flexible, Stretchable, and Spanning Silver Microelectrodes.* Science, 2009. **323**(5921): p. 1590-1593.

16. Schmidt, O.G. and N.Y. Jin-Phillipp, *Free-standing SiGe-based nanopipelines on Si (001) substrates.* Applied Physics Letters, 2001. **78**(21): p. 3310-3312.

17. Kalaitzidou, K. and A.J. Crosby, *Adaptive polymer particles.* Applied Physics Letters, 2008. **93**(4): p. -.

18. Wu, L.C. and Y.F. Chou, *On-wafer characterization of thermomechanical properties isotropic thin films deposited on anisotropic substrates.* Japanese Journal of Applied Physics, 2008. **47**(7): p. 5623-5629.

19. Freund, L.B., J.A. Floro, and E. Chason, *Extensions of the Stoney formula for substrate curvature to configurations with thin substrates or large deformations.* Applied Physics Letters, 1999. **74**(14): p. 1987-1989.

20. Zhang, Y. and Y.P. Zhao, *Applicability range of Stoney's formula and modified formulas for a film/substrate bilayer.* Journal of Applied Physics, 2006. **99**(5): p. -.

21. Hubbard, T. and J. Wylde. *Residual strain and resultant postrelease deflection of surface micromachined structures*. 2000: Amer Inst Physics.

22. Clyne, T.W., *Residual stresses in surface coatings and their effects on interfacial debonding.* Interfacial Effects in Particulate, Fibrous and Layered Composite Materials, 1996. **116-**: p. 307-330.

23. Luzinov, I., S. Minko, and V.V. Tsukruk, *Adaptive and responsive surfaces through controlled reorganization of interfacial polymer layers.* Progress in Polymer Science, 2004. **29**(7): p. 635-698.

24. Luzinov, I., S. Minko, and V.V. Tsukruk, *Responsive brush layers: from tailored gradients to reversibly assembled nanoparticles.* Soft Matter, 2008. **4**(4): p. 714-725.

25. Sheparovych, R., M. Motornov, and S. Minko, *Low Adhesive Surfaces that Adapt to Changing Environments.* Advanced Materials, 2009. **21**(18): p. 1840-+.

26. You, Y.Z., et al., *Multi-responsive carbon nanotube gel prepared via ultrasound-induced assembly.* Journal of Materials Chemistry, 2009. **19**(41): p. 7656-7660.

27. Gao, K., et al., *Influences of Substrate and Annealing on the Structural and Optical Properties and Photoluminescence of Nanocrystalline ZnO Films Prepared by Plasma Assisted Pulsed Laser Deposition.* Journal of Physical Chemistry C, 2009. **113**(44): p. 19139-19144.

28. Holmes, D.P. and A.J. Crosby, *Snapping surfaces.* Advanced Materials, 2007. **19**(21): p. 3589-+.

29. Mano, J.F., *Stimuli-responsive polymeric systems for biomedical applications.* Advanced Engineering Materials, 2008. **10**(6): p. 515-527.

30. Regan, B.C., et al., *Carbon nanotubes as nanoscale mass conveyors.* Nature, 2004. **428**(6986): p. 924-927.

31. Mata, A., A.J. Fleischman, and S. Roy, *Characterization of polydimethylsiloxane (PDMS) properties for biomedical micro/nanosystems.* Biomedical Microdevices, 2005. **7**(4): p. 281-293.

32. Raez, J., I. Manners, and M.A. Winnik, *Fiberlike structures from the self-assembly of a highly asymmetric poly(ferrocenyldimethylsilane-b-dimethylsiloxane) in dilute solution.* Langmuir, 2002. **18**(19): p. 7229-7239.

33. Schmaljohann, D., *Thermo- and pH-responsive polymers in drug delivery.* Advanced Drug Delivery Reviews, 2006. **58**(15): p. 1655-1670.

34. Brandrup, J., et al., eds. *Polymer Handbook*. 4th Edition ed. 2005, John Wiley & Sons.

35. Fortin, J. and T.M. Lu, *Chemical Vapor Deposition Polymerization - The Growth and Properties of Parylene Thin Films*. 2004, Norwell, MA: Kluwer Academic Publishers Group.

36. *Silicon Carbide*. The Columbia Encyclopedia 2008 [cited 2010 15 Mar]; Sixth:[Available from: http://www.encyclopedia.com/doc/1E1-siliconc.html.

37. Bhatnagar, M. and B.J. Baliga, *Comparison of 6h-Sic, 3c-Sic, and Si for Power Devices.* Ieee Transactions on Electron Devices, 1993. **40**(3): p. 645-655.

38. *Properties of Silicon Carbide*. Emis Datareviews Series No. 13, ed. G.L. Harris. 1995, London, UK: INSPEC, the Institution of Electrical Engineers.

39. Shih, T.K., et al., *Fabrication of optical gratings by shrinkage of a rubber material.* Thin Solid Films, 2008. **516**(16): p. 5339-5343.

40. Lotters, J.C., et al., *The mechanical properties of the rubber elastic polymer polydimethylsiloxane for sensor applications.* Journal of Micromechanics and Microengineering, 1997. **7**(3): p. 145-147.

41. Thangawng, A.L., et al., *An ultra-thin PDMS membrane as a bio/micro-nano interface: fabrication and characterization.* Biomedical Microdevices, 2007. **9**(4): p. 587-595.

42. *UVO Cleaner ® - Ozone cleaning device*. Jelight Company Inc. 2010 [cited 2010 20 January]; Available from: http://www.jelight.com/uvo-ozone-cleaning.php.

43. *Unaxis PECVD*. Nanotechnology Research Center 2010 [cited 2010 15 January]; Available from: http://grover.mirc.gatech.edu/equipment/textInstructions.php?id=112.

44. *Sputter Coater*. Center for Nanostructure Characterization 2010 [cited 2010 15 January]; Available from: http://cncf.nanoscience.gatech.edu/equipment.htm.

45. *CVC Electron Beam Evaporator*. Nanotechnology Research Center 2010 [cited 2010 15 January]; Available from: http://grover.mirc.gatech.edu/equipment/textInstructions.php?id=30.

46. Tiaw, K.S., M.H. Hong, and S.H. Teoh, *Precision laser micro-processing of polymers.* Journal of Alloys and Compounds, 2008. **449**(1-2): p. 228-231.

47. Lee, S., E.V. Bordatchev, and M.J.F. Zeman, *Femtosecond laser micromachining of polyvinylidene fluoride (PVDF) based piezo films.* Journal of Micromechanics and Microengineering, 2008. **18**(4): p. -.

48. Gil, E.S. and S.A. Hudson, *Stimuli-reponsive polymers and their bioconjugates.* Progress in Polymer Science, 2004. **29**(12): p. 1173-1222.

49. Philippova, O.E., et al., *pH-responsive gels of hydrophobically modified poly(acrylic acid).* Macromolecules, 1997. **30**(26): p. 8278-8285.

50. Pinkrah, V.T., et al., *Physicochemical properties of poly(N-isopropylacrylamide-co-4-vinylpyridine) cationic polyelectrolyte colloidal microgels.* Langmuir, 2003. **19**(3): p. 585-590.

51. Simnick, A.J., et al., *Biomedical and biotechnological applications of elastin-like polypeptides.* Polymer Reviews, 2007. **47**(1): p. 121-154.

52. Xia, F., et al., *Smart responsive surfaces switching reversibly between super-hydrophobicity and super-hydrophilicity.* Soft Matter, 2009. **5**(2): p. 275-281.

53. Lahann, J., et al., *A reversibly switching surface.* Science, 2003. **299**(5605): p. 371-374.

54. Irvin, J.A., et al., *Low-oxidation-potential conducting polymers derived from 3,4-ethylenedioxythiophene and dialkoxybenzenes.* Journal of Polymer Science Part a-Polymer Chemistry, 2001. **39**(13): p. 2164-2178.

55. Zhang, J.L., et al., *Reversible superhydrophobicity to superhydrophilicity transition by extending and unloading an elastic polyamide.* Macromolecular Rapid Communications, 2005. **26**(6): p. 477-480.

56. Sundararajan, S. and B. Bhushan, *Development of AFM-based techniques to measure mechanical properties of nanoscale structures.* Sensors and Actuators a-Physical, 2002. **101**(3): p. 338-351.

57. Sharpe, W.N., B. Yuan, and R.L. Edwards, *A new technique for measuring the mechanical properties of thin films.* Journal of Microelectromechanical Systems, 1997. **6**(3): p. 193-199.

58. Son, D., J.H. Jeong, and D. Kwon, *Film-thickness considerations in microcantilever-beam test in measuring mechanical properties of metal thin film.* Thin Solid Films, 2003. **437**(1-2): p. 182-187.

59. Retajczyk, T.F. and A.K. Sinha, *ELASTIC STIFFNESS AND THERMAL-EXPANSION COEFFICIENTS OF VARIOUS REFRACTORY SILICIDES AND SILICON-NITRIDE FILMS.* Thin Solid Films, 1980. **70**(2): p. 241-247.

60. Vivino, M. *NIH Image Engineering*. [cited 2010 20 March]; Available from: http://rsb.info.nih.gov/nih-image/more-docs/Engineering/ImgEngr.html.

61. Kost, J. and R. Langer, *Responsive polymeric delivery systems.* Advanced Drug Delivery Reviews, 2001. **46**(1-3): p. 125-148.

62. Allen, M.G. and S.D. Senturia, *MICROFABRICATED STRUCTURES FOR THE MEASUREMENT OF ADHESION AND MECHANICAL-PROPERTIES OF POLYMER-FILMS.* Abstracts of Papers of the American Chemical Society, 1987. **193**: p. 166-PMSE.

63. Xiao, J., et al., *Stretchable and compressible thin films of stiff materials on compliant wavy substrates.* Applied Physics Letters, 2008. **93**(1): p. 3.

64. Zeng, S., et al. *Systematic Design Method For Information Modeling in CAD/CAE*. in *ASME 2003 Design Engineering Technical Conferences and 23rd Computers and Information in Engineering Conference*. 2003. Chicago, IL.

65. Hirtz, J., et al., *A functional basis for engineering design: Reconciling and evolving previous efforts.* Research in Engineering Design-Theory Applications and Concurrent Engineering, 2002. **13**(2): p. 65-82.

66. Pahl, G., et al., *Engineering Design: A Systematic Approach.* . 3rd ed. ed. 2007: London: Springer-Verlag.

67. Song, J., et al., *Mechanics of stretchable inorganic electronic materials.* Journal of Vacuum Science & Technology A, 2009. **27**(5): p. 1107-1125.

68. Yu, C.J., et al., *A stretchable temperature sensor based on elastically buckled thin film devices on elastomeric substrates.* Applied Physics Letters, 2009. **95**(14): p. -.

69. Mansour, S.A., *Effect of extensional cyclic strain on the mechanical and physico-mechanical properties of PVC-NBR/graphite composites.* Express Polymer Letters, 2008. **2**(12): p. 836-845.

70. Baek, J.B., C.B. Lyons, and L.S. Tan, *Grafting of vapor-grown carbon nanofibers via in-situ polycondensation of 3-phenoxybenzoic acid in poly(phosphoric acid).* Macromolecules, 2004. **37**(22): p. 8278-8285.

71. Endo, M., et al., *Vapor-grown carbon fibers (VGCFs) - Basic properties and their battery applications.* Carbon, 2001. **39**(9): p. 1287-1297.

72. Lafdi, K., et al., *Effect of carbon nanofiber-matrix adhesion on polymeric nanocomposite properties - Part II.* Journal of Nanomaterials, 2008: p. -.

73. Khosla, A. and B.L. Gray, *Preparation, characterization and micromolding of multi-walled carbon nanotube polydimethylsiloxane conducting nanocomposite polymer.* Materials Letters, 2009. **63**(13-14): p. 1203-1206.

74. Mironov, V.S., et al., *Comparison of electrical conductivity data obtained by four-electrode and four-point probe methods for graphite-based polymer composites.* Polymer Testing, 2007. **26**(4): p. 547-555.

75. Kim, S.M. and K.J. Kim, *Palladium buffer-layered high performance ionic polymer-metal composites.* Smart Materials & Structures, 2008. **17**(3): p. -.

76. Pyo, M. and J.H. Hwang, *Conductivity changes of dodecylbezensulfonic acid-doped polyaniline during pressure loading/unloading.* Synthetic Metals, 2009. **159**(7-8): p. 700-704.

77. Leng, J.S., et al., *Electroactive thermoset shape memory polymer nanocomposite filled with nanocarbon powders.* Smart Materials & Structures, 2009. **18**(7): p. -